Role of the environmental spectrum in the decoherence and dissipation of a quantum Brownian particle

Pro gradu -tutkielma
Turun yliopisto
Fysiikan laitos
Teoreettinen fysiikka
2008

Janika Paavola

Tarkastajat:
dos. Sabrina Maniscalco
prof. Kalle-Antti Suominen

TURUN YLIOPISTO
Fysiikan laitos
PAAVOLA, JANIKA: Role of the environmental spectrum in the decoherence and dissipation of a quantum Brownian particle
Pro gradu -tutkielma, 60 sivua
Teoreettinen fysiikka
Kesäkuu 2008

Tässä tutkielmassa käsitellään avoimen eli ympäristönsä kanssa vuorovaikuttavan kvanttisysteemin dynamiikkaa. Painopiste on unitaarievoluution sijaan dekoherenssin ja dissipaation kuvauksessa. Nämä kaksi ilmiötä aiheuttavat kvanttimekaanisen superpositio- ja kietoutuneen tilan hajoamisen. Dekoherenssi ja dissipaatio kvanttisysteemeissä johtuvat väistämättömästä vuorovaikutuksesta ympäristön kanssa. Dekoherenssin ja dissipaation tarkka dynamiikka riippuu ympäristön rakenteesta.

Mallisysteeminä tässä tutkielmassa on harmonisessa potentiaalissa liikkuva hiukkanen, joka vuorovaikuttaa termisen ympäristön kanssa eli niin sanottu QBM-malli. Olen johtanut tälle systeemille liikeyhtälön heikon kytkennän approksimaatiossa käyttäen apuna ei-Markovista teoriaa, joka mallintaa ympäristön ja systeemin vuorovaikutusta. Liikeyhtälöstä saatavat ajasta riippuvat kertoimet $\Delta(t)$ ja $\gamma(t)$ ilmaisevat dekoherenssin ja dissipaation nopeuden.

Olen tehnyt vertailevan teoreettisen tutkimuksen dekoherenssivakioiden $\Delta(t)$ ja $\gamma(t)$ dynamiikasta kolmella eri ympäristömallilla sekä korkeissa että matalissa lämpötiloissa. Tutkin myös miten systeemin keskimääräinen energia käyttäytyy sekä lyhyillä että pitkillä ajanjaksoilla. Tulokset antavat yleiskuvan dekoherenssi- ja dissipaatioilmiöiden nopeuteen vaikuttavista tekijöistä. Tämä tieto on hyödyksi, kun pyritään kehittämään kvanttitietokoneita, joiden toiminta perustuu superpositiolla ja kietoutuneilla kvanttitiloilla operointiin.

Nyt saatuja tuloksia voidaan myöhemmin hyödyntää tutkittaessa miten superpositio- tai kietoutuneita tiloja voidaan suojata ympäristön haittavaikutuksilta suorittamalla ei-selektiivisiä mittauksia.

Asiasanat: Kvanttimekaniikka, avoimet kvanttisysteemit, dekoherenssi, dissipaatio

Contents

Preface

In this thesis we examine how the interaction with the environment affects the dynamics of a quantum system. The quantum system under scrutiny is the commonly used quantum harmonic oscillator with damping induced by the coupling to a thermal environment. We use theoretical methods to first derive an approximate equation of motion for the system of interest. We then discuss the exact equation of motion and its solution. Finally we present our main result, a comparative study on the effect that different environments have on the dynamics of the quantum harmonic oscillator. To this aim we introduce three different environments and compare the dynamics of the time-dependent coefficients characterizing the effect of the environment on the system. We also study how the environment induced heating of the system oscillator varies with different environments.

The thesis is structured in the following way. In the first chapter a general introduction to the topic of open quantum systems is given and the open quantum system model used throughout the thesis, namely, the quantum Brownian motion model is presented. In chapter 2 we derive an equation of motion for this model. The derivation relies on some approximations, but an exact equation of motion is also given for reference. We then briefly discuss the exact solution to the equation of motion of a quantum Brownian particle. Chapter 3 focuses on the microscopic interaction between the system and the environment, and discusses the different physical quantities playing a role in the modeling of the interaction. In chapter 4 we present our results on the time-dependent decay rates appearing in the equation of motion.

These decay rates characterize the dissipative dynamics of the quantum state of the system. More results characterizing the heating of the quantum Brownian particle due to the interaction with a thermal reservoir are presented in chapter 5. The final chapter 6 contains the conclusions.

Acknowledgements

This work started when I was a summer trainee in the department of Physics, Quantum optics group in Turku in the summer of 2007. I would like to express my hearty thanks to the whole group for making me feel welcome in this international community of physicists. I thank the group leader Prof. Kalle-Antti Suominen for discussions and providing me the opportunity to begin my scientific career in such an international group. Because of this I have had the chance to present my work to some of the visitors we have had during my time in the group. These people include Prof. Giuseppe Compagno, Dr. Heinz-Peter Breuer and Dr. Barry Garraway. I would like to thank them for discussions and for the opportunity to improve my skills in presenting my results. I would like to express my deepest gratitude to Dos. Sabrina Maniscalco and Dos. Jyrki Piilo who have tirelessly guided me in my thesis work by offering many advice and discussions. I would also like to thank Kari Härkönen and Otto Vainio, who share an office with me, especially for helping me with all sorts of technical problems. Finally, I would like to thank my fiancé Ville for being an ingenious source of inspiration, and the rest of my family and relatives for their support. I acknowledge financial support from the Academy of Finland (Project No. 115982).

Chapter 1

Open systems in quantum mechanics

1.1 Introduction

Textbook approach to quantum mechanics introduces the Schrödinger equation

$$i\frac{d}{dt}|\psi(t)\rangle = H|\psi(t)\rangle \tag{1.1}$$

that describes the evolution of the system whose state is represented by the state vector $|\psi\rangle$ with Hamiltonian H. Here we have set $\hbar = 1$ and will use the same natural units throughout the thesis. The time evolution of $|\psi\rangle$ is given by the unitary operator $U_t = e^{-itH}$ as

$$|\psi(t)\rangle = U_t|\psi(t)\rangle. \tag{1.2}$$

These equations describe the dynamics of systems that do not interact nor are entangled with other systems. Systems like this are defined to be closed. A system can never be completely isolated from its surroundings but inevitable interactions with the environment occur, e.g., via heat transfer. In this respect all physical quantum systems are open, while sometimes it is useful and well argued to use the closed system approach as a reasonable approximation.

Research in open quantum systems has been fueled by the efforts to develop quantum information devices that can utilize the potential emerging from two peculiar features of quantum systems, namely entanglement and the existence of quantum superposition. Entanglement is a quantum correlation between two parts of a composite system. In addition to being a key concept in the theoretical description of the quantum world, entanglement is also a necessary ingredient in quantum information devices. Entanglement and quantum superposition can be used to implement quantum information processing that, in some cases, is hugely more efficient than classical information processing [1].

Entanglement and quantum superpositions deteriorate when a quantum system interacts with the environment. The coupling to the environment transforms quantum superpositions into classical statistical mixtures in a process called environment induced decoherence [2]. This transformation is also known as quantum to classical transition. Also the entanglement between, e.g., two qubits (i.e., the quantum counterparts of classical bits), is destroyed by the noise induced by the system-environment coupling. The environment is typically described by a spectral distribution function. Different physical contexts, e.g., solid state physics, photonic band gap materials and quantum optics, are characterized by different spectral distributions. By conducting a comparative study on the effect different environments have on quantum state deterioration in open systems, we can understand how and to which extent the important quantum properties could be used in technologies. It has been proven that the more macroscopic and distinguishable are the components of a quantum superposition, the faster is the environment induced decoherence [3]. In this context it is possible to understand, why there exists no superpositions of macroscopic objects like the one in Schrödinger's cat paradox [4]: the size of the system is huge and therefore decoherence takes place almost instantaneously.

The description of the total closed system-environment dynamics is typically a virtually impossible task due to the large, generally infinite, number of degrees of

freedom of the environment. Moreover, very often we are not interested in the dynamics of the environment but rather on its effects on the reduced system dynamics. A common approach in studying the dynamics of open systems is therefore first to write an equation of motion for the total closed system (i.e., system plus the environment) and then to derive an equation of motion for the reduced system by tracing over the environmental degrees of freedom. This means that the evolution operator is not unitary anymore, as was the case for the Schrödinger equation for closed systems. The reduced density operator of the system is defined as $\rho_S = \mathrm{tr}_E\{\rho\}$, where ρ is the density operator of the total system and tr_E indicates the partial trace over environmental degrees of freedom [5].

In the theoretical study of open quantum systems, the system and the environment can be modeled in various ways. In this thesis we use the model consisting of a damped quantum harmonic oscillator as our system and a chain of quantum harmonic oscillators linearly coupled to this system as our environment. This is also known as the quantum Brownian motion model.

1.2 Quantum Brownian motion

In this section we introduce the physical system whose dynamics is the object of this thesis. This system is quantum Brownian motion in a harmonic potential. Quantum Brownian motion (QBM) is a paradigmatic open quantum system model, describing a particle (quantum Brownian particle) with mass m and position coordinate x, moving in a harmonic potential $V(x)$ and coupled to the environment. The Hamiltonian for the quantum Brownian particle is

$$H_S = \frac{\hat{p}^2}{2m} + V(\hat{x}), \tag{1.3}$$

where $\hat{p}$ is the particle momentum operator and $\hat{x}$ is the position operator [5]. In the following we will focus on the case of a quadratic potential, i.e. $V(\hat{x}) = \frac{1}{2}m\omega_0^2\hat{x}^2$. In this case, essentially, the QBM model describes a quantum harmonic oscillator

of frequency ω_0 with damping caused by the coupling with the environment. QBM is one of the few open quantum systems models that can be solved analytically, being therefore a valuable tool in many physical contexts. One of the applications of QBM is the description of a quantum electromagnetic field propagating in a linear dielectric medium [6]. Quantum Brownian motion also describes the dynamics of a particle interacting with a quantum field in dipole approximation [7], a trapped ion for example. In addition to these quantum optical applications, the QBM model is used in nuclear physics [8] and quantum chemistry [9].

Chapter 2

Dynamics of quantum Brownian motion

2.1 Introduction

This chapter focuses on the description of the theoretical approach used to investigate the dynamics of QBM in a harmonic potential. We will begin deriving the approximated master equation for the reduced density matrix using perturbation theory. For the sake of completeness also the exact master equation will then be presented and briefly discussed. Finally, we will introduce the solution of the master equation and discuss its features.

The derivation of the equation of motion for the reduced density operator, known as the master equation, is often a very difficult task. For this reason often one performs a number of approximations that turn out to be reasonable in many physical contexts. This is the approach followed also in this thesis. To find the equation of motion for QBM, we fist assume that at some initial time t_0 the system and the environment are uncorrelated and that the environment is stationary, that is, it does not change with time. Second, we make a weak coupling approximation or Born approximation, which limits the validity of the master equation to systems

where the interaction with the environment is not very strong. This is a reasonable approximation for most applications, for example, in the case of trapped ions [10]. The third approximation is the secular approximation. This means neglecting terms that oscillate very rapidly compared to the timescale of the dynamics.

In the following we will examine in detail the microscopic derivation of the master equation and derive the condition of validity of these approximations.

2.2 Microscopic derivation of master equation - perturbative approach

2.2.1 General form for master equation

We begin considering the general derivation of the master equation for the reduced system density matrix starting from a microscopic description of the closed total system and assuming that the system and the environment are weakly coupled. We follow the derivation methods used in Ref. [5]. We begin with a total Hamiltonian

$$H = H_S + H_E + \alpha H_I,$$

where H_S, H_E and H_I are the Hamiltonians of the system, environment and interaction, respectively, and α is a dimensionless constant proportional to the strenght of the coupling between the system and the environment. It is convenient to use the interaction picture (denoted by tilde). The density operator in the interaction picture is given by

$$\tilde{\rho}(t) \equiv e^{it(H_S+H_E)}\rho(t)e^{-it(H_S+H_E)}. \tag{2.1}$$

The derivation starts from the interaction picture von Neumann equation

$$\frac{d}{dt}\tilde{\rho}(t) = -i\alpha[\tilde{H}_I(t), \tilde{\rho}(t)], \tag{2.2}$$

which can be formally integrated. This gives us the total density matrix

$$\tilde{\rho}(t) = \tilde{\rho}(0) - i\alpha \int_0^t [\tilde{H}_I(t'), \tilde{\rho}(t')]\, dt'. \tag{2.3}$$

Using recursively this expression we get the Dyson series

$$\begin{aligned}\tilde{\rho}(t) = \tilde{\rho}(0) - i\alpha \int_0^t [\tilde{H}_I(t'), \tilde{\rho}(0)]\, dt' + (-i\alpha)^2 \int_0^t \int_0^{t'} \left[\tilde{H}_I(t'), [\tilde{H}_I(t''), \tilde{\rho}(0)]\right]\, dt''\, dt' \\ + (-i\alpha)^3 \int_0^t \int_0^{t'} \int_0^{t''} \left[\tilde{H}_I(t'), \left[\tilde{H}(t''), [\tilde{H}(t'''), \tilde{\rho}(0)]\right]\right]\, dt'''\, dt''\, dt' + \ldots\end{aligned} \tag{2.4}$$

Taking the derivative of equation (2.4) and neglecting terms that are higher than second order in the coupling constant yields

$$\frac{d}{dt}\tilde{\rho}(t) = -i\alpha[\tilde{H}_I(t), \tilde{\rho}(0)] - \alpha^2 \int_0^t \left[\tilde{H}_I(t), [\tilde{H}_I(t'), \tilde{\rho}(0)]\right]\, dt'. \tag{2.5}$$

This approximation is the Born or weak coupling approximation. The terms neglected are $\mathcal{O}(\alpha^3)$ and are therefore extremely small, given that we had assumed a weak coupling, that is, a small value for α. So far, all the equations are valid for the closed total system. Open system dynamics emerge, when we trace over the environmental degrees of freedom obtaining an equation for the reduced system:

$$\frac{d}{dt}\tilde{\rho}_S(t) = -i\alpha \mathrm{tr}_E\{[\tilde{H}_I(t), \tilde{\rho}(0)]\} + (-i\alpha)^2 \int_0^t \mathrm{tr}_E\{[\tilde{H}_I(t), [\tilde{H}_I(t'), \tilde{\rho}(0)]]\}\, dt'. \tag{2.6}$$

In order to proceed further, few assumptions are made. First, we assume that at initial time $t = 0$ the system and the environment are uncorrelated, that is

$$\tilde{\rho}(0) = \tilde{\rho}_S(0) \otimes \tilde{\rho}_E(0). \tag{2.7}$$

Second, we assume that the environment is stationary. By definition this means that $[H_E, \rho_E] = 0$, where ρ_E is the density matrix of the environment. From the stationarity assumption it also follows that $\tilde{\rho}_E(0) = \rho_E$. By substituting Eq. (2.7) into Eq. (2.6) we get

$$\frac{d}{dt}\tilde{\rho}_S(t) = -i\alpha \mathrm{tr}_E\{[\tilde{H}_I(t), \tilde{\rho}_S(0) \otimes \rho_E]\} - \alpha^2 \int_0^t \mathrm{tr}_E\{[\tilde{H}_I(t), [\tilde{H}_I(t'), \tilde{\rho}_S(0) \otimes \rho_E]]\}\, dt'. \tag{2.8}$$

The integral form of Eq. (2.8) is

$$\tilde{\rho}_S(t) - \tilde{\rho}_S(0) = -i\alpha \int_0^t \mathrm{tr}_E\{[\tilde{H}_I(t'), \tilde{\rho}_S(0) \otimes \rho_E]\}\, dt' + \mathcal{O}(\alpha^2). \tag{2.9}$$

From this expression, $\tilde{\rho}_S(0)$ can be solved and substituted into Eq. (2.8). This leads to the following perturbative master equation for the system S

$$\begin{aligned} \frac{d}{dt}\tilde{\rho}_S(t) = &-i\alpha \mathrm{tr}_E\{[\tilde{H}_I(t), \tilde{\rho}_S(t) \otimes \rho_E]\} \\ &+ \alpha^2 \int_0^t \mathrm{tr}_E\{[\tilde{H}_I(t), \mathrm{tr}_E\{[\tilde{H}_I(t'), \tilde{\rho}_S(t) \otimes \rho_E]\} \otimes \rho_E]\}\, dt' \\ &- \alpha^2 \int_0^t \mathrm{tr}_E\{\big[\tilde{H}_I(t), [\tilde{H}_I(t'), \tilde{\rho}_S(t) \otimes \rho_E]\big]\}\, dt'. \end{aligned} \tag{2.10}$$

This equation is known as *the Redfield equation*. To summarize, it was obtained by using perturbation theory up to the second order in the coupling constant and assuming a factorized initial state and a stationary environment. It is a very general form of master equation, since we have not specified anything about the system, environment or interaction Hamiltonians. The Redfield equation (2.10) is also local in time, meaning that the state of the system depends only on the current time t and not on the past time $t_1 < t$. The master equation, however, does depend on the initial state $\tilde{\rho}(0)$.

2.2.2 Specifying the system and the environment

We now have a general master equation in the second order perturbation theory. In order to proceed further, the system and environment Hamiltonians must be defined. We are examining the case of quantum Brownian motion in a harmonic potential, so the system is a harmonic oscillator with Hamiltonian given by Eq. (1.3). This Hamiltonian can also be written in the following form

$$H_S = \omega_0 \left(a^\dagger a + \frac{1}{2} \right), \tag{2.11}$$

where

$$a = \frac{(X + iP)}{\sqrt{2}} \tag{2.12}$$

$$a^\dagger = \frac{(X - iP)}{\sqrt{2}} \tag{2.13}$$

are the creation and annihilation operators, with commutation property $[a, a^\dagger] = 1$. X and P are the dimensionless position and momentum operators

$$X = \left(\frac{m\omega_0}{\hbar}\right)^{1/2} \hat{x} \tag{2.14}$$

$$P = \left(\frac{1}{m\hbar\omega_0}\right)^{1/2} \hat{p}. \tag{2.15}$$

The environment is a heat bath modeled as an infinite chain of harmonic oscillators with the Hamiltonian

$$H_E = \sum_{n=0}^{\infty} \omega_n \left(b_n^\dagger b_n + \frac{1}{2}\right), \tag{2.16}$$

where $b_n^\dagger$, b_n and ω_n are the the creation operator, annihilation operator and the frequency of the nth oscillator, respectively. An environment with infinite degrees of freedom and in thermal equilibrium, such as in our case, is usually called a reservoir. The system and the reservoir are coupled linearly via the position operators, X and $\hat{x}_n$ for the system and reservoir oscillators, respectively, so that the interaction Hamiltonian is

$$H_I = X \sum_n k_n \hat{x}_n = \frac{1}{\sqrt{2}}(a + a^\dagger) \sum_n k_n \sqrt{\frac{1}{2\omega_n}}(b_n + b_n^\dagger). \tag{2.17}$$

Here k_n measures the coupling between each reservoir mode and the system oscillator. An interaction of this type yields a renormalization of the potential $V(\hat{x})$. To compensate for this renormalization, we include one extra term to the total Hamiltonian. This counter term reads

$$H_c = \hat{x}^2 \sum_n \frac{k_n^2}{2m_n\omega_n^2}. \tag{2.18}$$

With this adjustment we have as a system Hamiltonian $\bar{H}_S = \frac{p^2}{2m} + V_c(\hat{x})$, with

$$V_c(\hat{x}) = V(\hat{x}) + \hat{x}^2 \sum_n \frac{k_n^2}{2m_n\omega_n^2}. \tag{2.19}$$

Eigenoperators

In order to proceed with the derivation of the master equation it is desirable to express the interaction Hamiltonian H_I in terms of the eigenoperators of the system Hamiltonian, because in this way the transformation to the interaction picture becomes much easier [5]. An eigenoperator $S(\omega)$ is defined for a generic operator S with the help of the eigenvalues ε of H_S and the projections $\Pi(\varepsilon)$ onto the eigenspace corresponding to ε

$$S(\omega) = \sum_{\varepsilon' - \varepsilon = \omega} \Pi(\varepsilon) S \Pi(\varepsilon'). \tag{2.20}$$

One of the properties of eigenoperators is that

$$[H_S, S(\omega)] = -\omega S(\omega), \tag{2.21}$$

$$[H_S, S^\dagger(\omega)] = \omega S^\dagger(\omega). \tag{2.22}$$

Another important property allows us to express in a simple way the eigenoperators in the interaction picture:

$$\tilde{S}(\omega) = e^{iH_S t} S(\omega) e^{-iH_S t} = e^{-i\omega t} S(\omega), \tag{2.23}$$

$$\tilde{S}^\dagger(\omega) = e^{iH_S t} S^\dagger(\omega) e^{-iH_S t} = e^{i\omega t} S^\dagger(\omega). \tag{2.24}$$

From Eqs. (2.21) and (2.22) it can be easily checked that a and $a^\dagger$ are the eigenoperators of H_S, since, for example, $[H_S, a] = -\omega_0 a$. Therefore a and $a^\dagger$ in the interaction picture are simply given by

$$\begin{aligned} \tilde{a}(t) &\equiv e^{iH_S t} a e^{-iH_S t} = e^{-i\omega_0 t} a \\ \tilde{a}^\dagger(t) &\equiv e^{iH_S t} a^\dagger e^{+iH_S t} = e^{i\omega_0 t} a^\dagger. \end{aligned} \tag{2.25}$$

With the help of the equations above we can express the interaction Hamiltonian in the interaction picture as follows

$$\tilde{H}_I(t) = \frac{1}{\sqrt{2}} (\tilde{a} + \tilde{a}^\dagger) \otimes \tilde{E}(t) = \frac{1}{\sqrt{2}} (e^{-i\omega_0 t} a + e^{i\omega_0 t} a^\dagger) \otimes \tilde{E}(t), \tag{2.26}$$

where we have

$$\tilde{E}(t) = \sum_n k_n \frac{1}{\sqrt{2\omega_n}} \left[b_n(t) + b_n^\dagger(t) \right]. \tag{2.27}$$

The form of the master equation given in Eq. (2.10) can be simplified in the case of a thermal reservoir at temperature T described by a density operator of the form

$$\rho_E = \frac{1}{Z_B} \exp\left(-\sum_n \frac{\omega_n b_n^\dagger b_n}{k_B T} \right), \tag{2.28}$$

where k_B is the Boltzmann constant and Z_B is the partition function. From this it follows that

$$\mathrm{tr}_E\{[\tilde{H}_I(t), \tilde{\rho}_S(t) \otimes \rho_E]\} = 0.$$

Therefore the first two terms of the Redfield equation (2.10) vanish and we are left with the following master equation

$$\frac{d}{dt}\tilde{\rho}_S(t) = -\alpha^2 \int_0^t \mathrm{tr}_E\{\left[\tilde{H}_I(t), [\tilde{H}_I(t'), \tilde{\rho}_S(t) \otimes \rho_E]\right]\} dt'. \tag{2.29}$$

Inserting Eq. (2.26) into Eq. (2.29) gives

$$\begin{aligned} \frac{d}{dt}\tilde{\rho}_S(t) = \frac{\alpha^2}{2} \int_0^t \Big\{ & \mathrm{tr}_E\{\tilde{E}(t')\rho_E \tilde{E}(t)\}[\tilde{a}(t') + \tilde{a}^\dagger(t')]\tilde{\rho}_S(t)[\tilde{a}(t) + \tilde{a}^\dagger(t)] \\ & - \mathrm{tr}_E\{\tilde{E}(t)\tilde{E}(t')\rho_E\}[\tilde{a}(t) + \tilde{a}^\dagger(t)][\tilde{a}(t') + \tilde{a}^\dagger(t')]\tilde{\rho}_S(t) + h.c. \Big\} dt'. \end{aligned} \tag{2.30}$$

The two traces in the above equation are actually equivalent because the trace operation is cyclic, i.e., $\mathrm{tr}\{abc\} = \mathrm{tr}\{cab\} = \mathrm{tr}\{bca\}$. By defining a correlation function for the electric field operators as

$$\langle \tilde{E}(t)\tilde{E}(t') \rangle = \mathrm{tr}_E\{\tilde{E}(t)\tilde{E}(t')\rho_E\}, \tag{2.31}$$

and using the formalism given in Eq. (2.25) the master equation can be cast in the form

$$\begin{aligned} \frac{d}{dt}\tilde{\rho}_S(t) = \frac{\alpha^2}{2} \int_0^t \Big\{ & \langle \tilde{E}(t)\tilde{E}(t') \rangle \big[a\tilde{\rho}_S(t) a e^{-i\omega_0(t'+t)} + a\tilde{\rho}_S(t) a^\dagger e^{i\omega_0(t-t')} \\ & + a^\dagger \tilde{\rho}_S(t) a e^{-i\omega_0(t-t')} + a^\dagger \tilde{\rho}_S(t) a^\dagger e^{i\omega_0(t+t')} \big) \\ & - \langle \tilde{E}(t)\tilde{E}(t') \rangle \big(a a \tilde{\rho}_S(t) e^{-i\omega_0(t'+t)} + a a^\dagger \tilde{\rho}_S(t) e^{-i\omega_0(t-t')} \\ & + a^\dagger a \tilde{\rho}_S(t) e^{i\omega_0(t-t')} + a^\dagger a^\dagger \tilde{\rho}_S(t) e^{i\omega_0(t+t')} \big] + h.c. \Big\} dt'. \end{aligned} \tag{2.32}$$

Since the environment is stationary, it is invariant under time translations. Therefore we set $t - t' = s$ and obtain the following form for the master equation

$$\frac{d}{dt}\tilde{\rho}_S(t) = \frac{\alpha^2}{2}\Big\{\Gamma_{-\omega_0}(t)\big[a^\dagger\tilde{\rho}_S(t)a + a^\dagger\tilde{\rho}_S(t)a^\dagger e^{i\omega_0 2t} - aa^\dagger\tilde{\rho}_S(t) - a^\dagger a^\dagger\tilde{\rho}_S(t)e^{i\omega_0 2t}\big] + \Gamma_{\omega_0}(t)\big[a\tilde{\rho}_S(t)ae^{-i\omega_0 2t} + a\tilde{\rho}_S(t)a^\dagger - aa\tilde{\rho}_S(t)e^{-i\omega_0 2t} - a^\dagger a\tilde{\rho}_S(t)\big] + h.c.\Big\}, \tag{2.33}$$

where the time dependent coefficients $\Gamma_{\pm\omega_0}(t)$ are the one-sided Fourier-transforms of the reservoir correlation function

$$\Gamma_{\pm\omega_0}(t) = \frac{\alpha^2}{2}\int_0^t \langle\tilde{E}(s)\tilde{E}(0)\rangle e^{\pm i\omega_0 s}\, ds. \tag{2.34}$$

2.2.3 Calculating the reservoir correlation functions

The reservoir correlation functions that appear in the time dependent coefficients determine the behavior of the system as it evolves in time. In this subsection, we calculate the explicit form of these coefficients in the case of a thermal reservoir. Inserting Eq. (2.27) into Eq. (2.34) we get

$$\Gamma_{\pm\omega_0}(t) = \frac{\alpha^2}{2}\int_0^t e^{\pm i\omega_0 s}\sum_{n,m}\frac{k_n k_m}{2\sqrt{\omega_n\omega_m}}\big[\langle b_n(s)b_m\rangle + \langle b_n(s)b_m^\dagger\rangle + \langle b_n^\dagger(s)b_m\rangle + \langle b_n^\dagger(s)b_m^\dagger\rangle\big]\, ds. \tag{2.35}$$

Note that all operators are still in the interaction picture, but the tildes have been omitted to ease the notation. Also the notation $b_n(0) = b_n$ has been used. The environment density operator ρ_E is diagonal in the Fock state basis $|n_1, \ldots n_k, \ldots\rangle$, so terms of the form $\langle b_n(s)b_m\rangle$ differ from zero only when $n = m$. With the help of the thermal state density operator given in Eq. (2.28), the terms in brackets in Eq. (2.35) can be calculated. For example,

$$\langle b_n^\dagger(s)b_n\rangle = e^{i\omega_n s}\langle b_n^\dagger b_n\rangle = e^{i\omega_n s}\mathrm{tr}_E\{b_n^\dagger b_n\rho_E\} = e^{i\omega_n s}N(\omega_n), \tag{2.36}$$

where

$$N(\omega_n) = \frac{1}{\exp(\frac{\omega_n}{k_B T}) - 1} \tag{2.37}$$

is the Planck distribution, that is, the mean number of quanta in a mode with frequency ω_n of the thermal reservoir at temperature T. Similarly,

$$\langle b_n(s) b_n^\dagger \rangle = e^{-i\omega_n s}[N(\omega_n) + 1], \tag{2.38}$$

while all the other terms are zero. The time-dependent coefficients thus obtain the form

$$\Gamma_{\pm\omega_0}(t) = \frac{\alpha^2}{2} \int_0^t \sum_n \frac{k_n^2}{2\omega_n} \left\{ e^{i\omega_n s} N(\omega_n) + e^{-i\omega_n s}[N(\omega_n) + 1] \right\} e^{\pm i\omega_0 s}\, ds. \tag{2.39}$$

Continuum of frequencies

For a three dimensional electromagnetic field the coupling strength between each individual environment oscillator mode and the system oscillator k_n can be given in the form

$$k_n = \sqrt{\frac{4\pi\hbar\omega_n^2}{V}}, \tag{2.40}$$

where V has the units of a volume [12]. We now pass to a continuum of frequencies by replacing the sum with the corresponding integral:

$$\frac{1}{V} \sum_n \longrightarrow \int \frac{d^3k}{(2\pi)^3}. \tag{2.41}$$

In spherical coordinates the volume element is $d^3k = k^2 dk \sin\theta d\theta d\Phi$, with $k = |\vec{k}| = \omega_n/c$, and hence we get the following result

$$\int \frac{d^3k}{(2\pi)^3} = \frac{1}{(2\pi)^3 c^3} \int_0^\infty d\omega_n \omega_n^2 \int d\Omega = \frac{1}{3\pi^2 c^3} \int_0^\infty d\omega_n \omega_n^2. \tag{2.42}$$

The integral $\int d\Omega$ is the integral over a solid state angle of the wave vector. When two possible states of polarization are taken into account, this integral yields $8\pi/3$, where we have used the relation

$$\int d\Omega \big(\delta_{ij} - \frac{k_i k_j}{k^2}\big) = \frac{8\pi}{3}. \tag{2.43}$$

The time dependent coefficients $\Gamma_\pm(t)$ now take the form

$$\Gamma_{\pm\omega_0}(t) = \frac{2}{3\pi c^3} \frac{\alpha^2}{2} \int_0^\infty d\omega \omega^3 \int_0^t ds \left\{ e^{i(\omega \pm \omega_0)s} N(\omega) + e^{-i(\omega \mp \omega_0)s}[N(\omega) + 1] \right\}. \tag{2.44}$$

For a generic spectrum one has

$$\sum_n k_n^2 \longrightarrow \int J(\omega)\, d\omega. \tag{2.45}$$

As can be seen from the calculations above,

$$J(\omega) = \frac{2}{3\pi c^3}\, \omega^3 \tag{2.46}$$

is the spectral density of the three dimensional electric field in free space. The aim of this thesis is to study the dynamics of a QBM using different types of environments, i.e., different spectral densities $J(\omega)$. The expression of the time-dependent coefficients in terms of a generic spectral distribution reads as follows

$$\Gamma_{\pm\omega_0}(t) = \frac{\alpha^2}{2} \int_0^t ds \int_0^\infty d\omega\, J(\omega) \left\{ e^{i(\omega \pm \omega_0)s} N(\omega) + e^{-i(\omega \mp \omega_0)s} [N(\omega)+1] \right\}. \tag{2.47}$$

Separating the real and imaginary parts of $\Gamma(t)$

We can express $\Gamma_{\omega_0}(t)$ as a sum of real and imaginary parts:

$$\Gamma_{\omega_0}(t) = \frac{1}{2}\gamma_{\omega_0}(t) + i\lambda_{\omega_0}(t), \tag{2.48}$$

where

$$\gamma_{\omega_0}(t) = \Gamma_{\omega_0}(t) + \Gamma^*_{\omega_0}(t) \tag{2.49}$$

$$\lambda_{\omega_0}(t) = \frac{1}{2i} \left[\Gamma_{\omega_0}(t) - \Gamma^*_{\omega_0}(t) \right]. \tag{2.50}$$

From Eq. (2.49) we obtain

$$\begin{aligned} \gamma_{\omega_0}(t) = \frac{\alpha^2}{2} \int_0^t ds \int_0^\infty d\omega\, J(\omega) \big[& e^{i(\omega+\omega_0)s} N(\omega) \\ & + e^{-i(\omega-\omega_0)s}(N(\omega)+1) + e^{-i(\omega+\omega_0)s} N(\omega) + e^{i(\omega-\omega_0)s}(N(\omega)+1) \big]. \end{aligned} \tag{2.51}$$

By using the addition formula for the cosine function we get

$$\begin{aligned} \gamma_{\omega_0}(t) = & \, 2 \int_0^t ds \int_0^\infty d\omega\, J(\omega) \left[N(\omega) + \frac{1}{2} \right] \cos(\omega s) \cos(\omega_0 s) \\ & + 2 \int_0^t ds \int_0^\infty d\omega\, \frac{J(\omega)}{2} \sin(\omega s) \sin(\omega_0 s), \end{aligned} \tag{2.52}$$

where α^2 has been incorporated in $J(\omega)$. We denote Eq. (2.52) as

$$\gamma_{\omega_0}(t) = \Delta(t) + \gamma(t), \tag{2.53}$$

where

$$\begin{aligned} \Delta(t) &= 2\int_0^t ds \int_0^\infty d\omega\, J(\omega) \left[N(\omega) + \frac{1}{2}\right] \cos(\omega s)\cos(\omega_0 s) \\ \gamma(t) &= 2\int_0^t ds \int_0^\infty d\omega\, \frac{J(\omega)}{2} \sin(\omega s)\sin(\omega_0 s). \end{aligned} \tag{2.54}$$

Following the same line of thinking we obtain the other time dependent coefficient

$$\gamma_{-\omega_0}(t) = \Delta(t) - \gamma(t). \tag{2.55}$$

Similarly we can express $\lambda_{\pm\omega_0}(t)$, defined by Eq. (2.50) as follows

$$\lambda_{\pm\omega_0}(t) = \Pi(t) \mp r(t), \tag{2.56}$$

where

$$\begin{aligned} r(t) &= \int_0^t ds \int_0^\infty d\omega\, \frac{J(\omega)}{2} \cos(\omega s)\sin(\omega_0 s) \\ \Pi(t) &= \int_0^t ds \int_0^\infty d\omega\, J(\omega)\,[N(\omega)+1] \sin(\omega s)\cos(\omega_0 s) \end{aligned} \tag{2.57}$$

The physical meaning of terms $\Delta(t)$, $\gamma(t)$, r(t) and $\Pi(t)$ is the following: $\gamma(t)$ is a damping term, while $\Delta(t)$ and $\Pi(t)$ are diffusive terms. The term r(t) is a frequency renormalization term [5].

2.2.4 Secular approximation

We can neglect the terms oscillating at frequency $2\omega_0$ in the master equation (2.35) since their contribution averages to zero for times $\omega_0 t \gg 1$. This is a common procedure in quantum optics. It is also known as the rotating wave approximation (RWA). We are left with the following master equation in the secular approximation

$$\frac{d}{dt}\rho_S(t) = \Gamma_{-\omega_0}(t)\left[a^\dagger \rho_S(t) a - a a^\dagger \rho_S(t)\right] + \Gamma_{\omega_0}(t)\left[a\rho_S(t)a^\dagger - a^\dagger a \rho_S(t)\right] + h.c. \tag{2.58}$$

By substituting γ and λ terms defined earlier, the master equation above can be divided into a part describing unitary evolution and a part giving the dissipative dynamics

$$\frac{d}{dt}\rho_S(t) = -i[H_{LS}, \rho_S(t)] + D[\rho_S(t)], \tag{2.59}$$

where the dissipation part is given by

$$D[\rho_S] = \gamma_{\omega_0}(t)\left[a^\dagger \rho_S a - \frac{1}{2}\{aa^\dagger, \rho_S\}\right] + \gamma_{-\omega_0}(t)\left[a\rho_S a^\dagger - \frac{1}{2}\{a^\dagger a, \rho_S\}\right] \tag{2.60}$$

and the unitary evolution is given with the help of the Lamb shift Hamiltonian H_{LS} as

$$\begin{aligned}
[H_{LS}, \rho_S] &= [\lambda_{\omega_0}(t)aa^\dagger + \lambda_{-\omega_0}(t)a^\dagger a, \rho_S] && (2.61)\\
&= (\Pi(t) - r(t))[aa^\dagger, \rho_S] + (\Pi(t) + r(t))[a^\dagger a, \rho_S]) && (2.62)\\
&= 2\Pi(t)[aa^\dagger, \rho_S]. && (2.63)
\end{aligned}$$

Here $[\,,]$ and $\{\,,\}$ represent the commutator and anti-commutator, respectively.

Decoherence dynamics

We are mostly interested in the decoherence dynamics, so we will neglect the unitary part of the master equation. After inserting Eqs. (2.53) and (2.55) into Eq. (2.60), the dissipator part of the master equation takes the form

$$\begin{aligned}
\frac{d}{dt}\rho_S(t) =& \frac{\Delta(t) - \gamma(t)}{2}\left(2a^\dagger \rho_S a - aa^\dagger \rho_S - \rho_S aa^\dagger\right)\\
&+ \frac{\Delta(t) + \gamma(t)}{2}\left(2a\rho_S a^\dagger - a^\dagger a\rho_S - \rho_S a^\dagger a\right),
\end{aligned} \tag{2.64}$$

where

$$\begin{aligned}
\Delta(t) &= 2\int_0^t ds \int_0^\infty d\omega\, J(\omega)\left[N(\omega) + \frac{1}{2}\right]\cos(\omega s)\cos(\omega_0 s) && (2.65)\\
\gamma(t) &= 2\int_0^t ds \int_0^\infty d\omega\, \frac{J(\omega)}{2}\sin(\omega s)\sin(\omega_0 s). && (2.66)
\end{aligned}$$

This equation is our starting point to investigate the decoherence and dissipation phenomena in QBM.

The quantum Brownian motion model, along with two-level system coupled to a bosonic reservoir, is one of the few models for which one can derive an exact master equation. It has been shown that, for certain class of observables, the perturbative solution derived in this thesis differs very little from the exact solution in the weak coupling limit [17]. It is thus well justified to use this approximative master equation as a starting point in the analysis of the dynamics of QBM.

2.3 Exact master equation

An exact master equation for QBM was first presented by Hu, Paz and Zhang in 1992 [16]. The authors used an influence functional path-integral method. After this, somewhat simpler methods of derivation have been introduced, for example in Ref. [17]. The derivation of the exact master equation is not conducted here. Instead, it is simply stated that if (i) the system and the environment are uncorrelated at the initial time $t = 0$, (ii) environment is stationary, that is $[H_E, \rho_E(0)] = 0$ and (iii) the expectation value of the environment is zero, e.g., in the case of a thermal reservoir, an exact master equation can be derived [11, 17] in the form

$$\begin{aligned}\frac{d}{dt}\rho_S(t) = -i\mathbf{H}_0^S\rho_S(t) - [\Delta(t)(\mathbf{X}^S)^2 - \Pi(t)\mathbf{X}^S\mathbf{P}^S \\ - \frac{i}{2}r(t)(\mathbf{X}^2)^S + i\gamma(t)\mathbf{X}^S\mathbf{P}^\Sigma]\rho_S(t).\end{aligned} \tag{2.67}$$

Bold letters indicate *superoperators*, i.e., operators that act on other operators. Superscript $S(\Sigma)$ indicates commutator (anticommutator) in the following way: $\mathbf{X}^S\rho = [X, \rho]$, $\mathbf{P}^\Sigma = \{P, \rho\}$. The time-dependent coefficients in the exact master equation to the second order in the coupling constant α, coincide with the coefficients

derived in our perturbative master equation, namely,

$$\begin{aligned}
\Delta(t) &= \int_0^t \kappa(\tau)\cos(\omega_0\tau)d\tau \\
\gamma(t) &= \int_0^t \mu(\tau)\sin(\omega_0\tau)d\tau \\
\Pi(t) &= \int_0^t \kappa(\tau)\sin(\omega_0\tau)d\tau \\
r(t) &= \int_0^t \mu(\tau)\cos(\omega_0\tau)d\tau,
\end{aligned}$$

with

$$\kappa(\tau) = \alpha^2\langle\{E(\tau), E(0)\}\rangle$$

and

$$\mu(\tau) = i\alpha^2\langle[E(\tau), E(0)]\rangle.$$

The exact master equation (2.67) is not limited to any specific coupling strength or temperature regime. It should be kept in mind, however, that the coefficients $\Delta(t)$, $\gamma(t)$, $\Pi(t)$ and $r(t)$ given above are the result of weak coupling approximation. It is possible to show that the exact and perturbative master equation have the same form in the weak coupling regime we are interested in [5].

2.4 Solution to the ME in terms of quantum characteristic function

In the literature there exists several approaches to the solution of the master equation (2.67). In the following we briefly review one of them, based on the algebraic properties of superoperators appearing in the QBM master equation [19]. The solution is given in terms of the quantum characteristic function (QCF) defined as

$$\chi_t(x,p) = \mathrm{tr}\{e^{-i(p\hat{X}-x\hat{P})}\rho\}. \tag{2.68}$$

From the knowledge of the QCF one can calculate the mean value of observables of interest such as, for example, the mean energy by means of the relations [18]

$$\langle X^n \rangle = (-i)^n \left(\frac{\partial^n}{\partial p^n} \chi(x,p) \right)_{x,p=0} \tag{2.69}$$

$$\langle P^n \rangle = (i)^n \left(\frac{\partial^n}{\partial x^n} \chi(x,p) \right)_{x,p=0}. \tag{2.70}$$

It has been demonstrated [19] that, in the weak coupling limit, the dynamics of the mean energy of the system oscillator are not affected by the RWA, so the master equation derived in this chapter, instead of the exact master equation (2.67), can be used to study the dynamics of the mean energy, provided that the system-reservoir coupling is weak enough. For the derivation of an analytical solution for the exact master equation, Eq. (2.67) can be recast into the following form

$$\frac{d}{dt}\rho_S(t) = [-i\bar{\mathbf{H}}_0^S(t) - \mathbf{D}_S(t) + \gamma(t)(\mathbf{N}+2)]\rho(t), \tag{2.71}$$

where

$$\mathbf{D}_S = \Delta(t)(\mathbf{X}^S)^2 + \Pi(t)\mathbf{X}^S\mathbf{P}^S \tag{2.72}$$

and

$$\bar{H}_0(t) = \frac{\hbar\omega_0}{2}\big[P^2 + X^2 - \frac{r(t)}{\omega_0}X^2 + \frac{\gamma(t)}{\omega_0}(XP+PX)\big]. \tag{2.73}$$

A formal solution is given by

$$\rho(t) = \mathbf{T}(t)\rho(0), \tag{2.74}$$

where the temporal evolution superoperator $\mathbf{T}$ is given by

$$\mathbf{T} = \exp_c \left\{ \int_0^t \big[-i\bar{\mathbf{H}}_0^S(t_1) - \mathbf{D}_S(t_1) + \gamma(t_1)(\mathbf{N}+2)\big] dt_1 \right\}. \tag{2.75}$$

Subscript c stands for Dyson chronological ordering.

2.4.1 Factorizing the temporal evolution superoperator

In order to obtain the solution, it is useful to try to manipulate $\mathbf{T}$ in order to get a form which is more convenient for the calculations. This has been done in a paper by

Intravaia *et al.*, where it has been shown that $\mathbf{T}(t)$ can be factorized in the following way [19]:

$$\mathbf{T}(t) = \mathbf{T}_S(t)\mathbf{T}_\Gamma(t)\mathbf{T}_D(t), \tag{2.76}$$

where

$$\begin{aligned}
\mathbf{T}_S(t) &= \exp_c\Big[-i\int_0^t \bar{\mathbf{H}}_0^S(t_1)dt_1\Big], && (2.77)\\
\mathbf{T}_\Gamma(t) &= \exp\Big[\frac{\Gamma(t)}{2}(\mathbf{N}+2)\Big], && (2.78)\\
\mathbf{T}_D(t) &= \exp\Big[-\int_0^t e^{\Gamma(t_1)}\bar{\mathbf{D}}(t_1)dt_1\Big], && (2.79)
\end{aligned}$$

with

$$\begin{aligned}
\Gamma(t) &= 2\int_0^t \gamma(t_1)dt_1, && (2.80)\\
\bar{\mathbf{D}}(t) &= \mathbf{T}_S^{-1}(t)\mathbf{D}_S(t)\mathbf{T}_S. && (2.81)
\end{aligned}$$

The factorization is done with the help of Feynman's rule and with certain algebraic properties of superoperators. Feynman's rule states that exponent functions that have sum of operators or superoperators as an argument can be factorized in the following way

$$\exp_c\Big[\int [A(t)+B(t)]dt\Big] = \exp_c\Big[\int A(t)dt\Big]\exp_c\Big[\int \bar{B}(t)dt\Big], \tag{2.82}$$

with

$$\bar{B}(t) = \Big(\exp_c\Big[\int A(t)dt\Big]\Big)^{-1} B(t)\Big(\exp_c\Big[\int A(t)dt\Big]\Big). \tag{2.83}$$

Next step is to examine how the temporal evolution superoperator $\mathbf{T}(t)$ acts on the initial density matrix. To make this process easier, we express the initial density matrix with the help of the QCF given in Eq. (2.68) as

$$\rho_S(0) = \frac{1}{2\pi}\int \chi_0(x,p)e^{-i(p\hat{X}-x\hat{P})}dxdp. \tag{2.84}$$

2.4.2 Applying $\mathbf{T}(t)$ to initial density matrix

If we now apply the time evolution superoperator to the initial density matrix given by the previous equation, we have

$$\rho_S(t) = \frac{1}{2\pi}\int \mathbf{T}_S(t)\mathbf{T}_\Gamma(t)\mathbf{T}_D(t)\chi_0(x,p)e^{-i(p\hat{X}-x\hat{P})}dxdp. \tag{2.85}$$

By calculating the effect of the operators $\mathbf{T}_S(t)$,$\mathbf{T}_\Gamma(t)$ and $\mathbf{T}_D(t)$ on $e^{-i(p\hat{X}-x\hat{P})}$, we obtain an expression for the density matrix at time t

$$\rho_S(t) = \frac{1}{2\pi}\int \chi_t(x,p)e^{-i(p\hat{X}-x\hat{P})}dxdp, \tag{2.86}$$

where

$$\chi_t(x,p) = \exp\left[-\begin{pmatrix}x & p\end{pmatrix}\bar{W}(t)\begin{pmatrix}x\\ p\end{pmatrix}\right]\chi_0\left[e^{-\Gamma(t)/2}R^{-1}(t)\begin{pmatrix}x\\ p\end{pmatrix}\right] \tag{2.87}$$

is the quantum characteristic function for the QBM. In this expression the matrix R is given by

$$R(t) = \begin{pmatrix}\cos\omega_0 t & \sin\omega_0 t\\ -\sin\omega_0 t & \cos\omega_0 t\end{pmatrix} \tag{2.88}$$

and

$$\bar{W}(t) = e^{-\Gamma(t)}[R^{-1}(t)]^T W(t) R^{-1}(t). \tag{2.89}$$

Moreover, we have

$$W(t) = \int_0^t e^{\Gamma(t_1)}\bar{M}(t_1)dt_1 \tag{2.90}$$

$$\bar{M}(t) = R^T(t)M(t)R(t) \tag{2.91}$$

$$M(t) = \begin{pmatrix}\Delta(t) & -\frac{\Pi(t)}{2}\\ -\frac{\Pi(t)}{2} & 0\end{pmatrix}. \tag{2.92}$$

2.4.3 Secular approximation

By performing the secular approximation, i.e., neglecting terms that are oscillating rapidly, we obtain a simpler form of the QCF for our system. In practice this is done

by neglecting the terms rotating at frequency $2\omega_0$ from the term $\bar{W}(t)$. If we insert into the definition of $\bar{W}(t)$ all the relevant variables given by (2.88) and (2.90)-(2.92) we obtain the following expression for the QCF,

$$\bar{W}(t) = e^{-\Gamma(t)} \int_0^t e^{\Gamma(t_1)} \left[\frac{\Delta(t_1)}{2} + \frac{\Delta(t_1)}{2} C_2(t-t_1) - \frac{\Pi(t_1)}{2} S_2(t-t_1) \right] dt_1, \quad (2.93)$$

with

$$C_2(t) = \begin{pmatrix} \cos 2\omega_0 t & -\sin 2\omega_0 t \\ -\sin 2\omega_0 t & -\cos 2\omega_0 t \end{pmatrix} \quad (2.94)$$

$$S_2(t) = \begin{pmatrix} \sin 2\omega_0 t & \cos 2\omega_0 t \\ \cos 2\omega_0 t & -\sin 2\omega_0 t \end{pmatrix}. \quad (2.95)$$

By performing the secular approximation, the matrices C_2 and S_2 average out to zero. Hence we are left with

$$\bar{W}(t) = e^{-\Gamma(t)} \int_0^t e^{\Gamma(t_1)} \frac{\Delta(t_1)}{2} dt_1 = \frac{\Delta_\Gamma(t)}{2}. \quad (2.96)$$

Inserting this expression into the solution of the exact master equation, we get

$$\rho_S^{\text{secular}}(t) = \frac{1}{2\pi} \int e^{-\Delta_\Gamma(t)(x^2+p^2)/2} \chi_0 \left[e^{-\Gamma(t)/2} R^{-1}(t) \begin{pmatrix} x \\ p \end{pmatrix} \right] e^{-i(p\hat{X} - x\hat{P})} dx dp, \quad (2.97)$$

with

$$\Delta_\Gamma(t) = e^{-\Gamma(t)} \int_0^t e^{\Gamma(t_1)} \Delta(t_1) dt_1. \quad (2.98)$$

The coefficient $\Gamma(t)$ is given by Eq. (2.80).

To sum up, the temporal evolution superoperator was first factorized to simplify the calculations. After that, the effect of the superoperator $\mathbf{T}(t)$ on the initial density matrix was calculated, yielding the solution to the exact master equation in terms of the quantum characteristic function.

2.5 Markovian vs. non-Markovian dynamics

One of the essential aspects of open quantum systems is the existence of memory effects between the system and the environment. Essentially, the unavoidable cou-

pling between a quantum system and its surrounding causes a flow of information and/or energy from the system to the environment. This information/energy can be fed back into the system due to the "environment-memory". This memory effect is characterized by the so called reservoir correlation time, which depends on both the properties of the system and the environment. When memory effects are taken into account, the future state of the reduced system is dependent on its past, and the dynamics is said to be non-Markovian.

2.5.1 Markovian approximation

In some quantum systems the reservoir correlation time is much shorter than the relaxation time. In this case one can perform the Markovian approximation that consists in neglecting the short time memory effects. Mathematically this amounts at replacing the upper limit of integrations in Eqs. (2.65)-(2.66) with infinity. The time dependent coefficients are therefore not time dependent anymore. They become constants reflecting the absence of feedback from the reservoir into the system.

In this thesis the main interest is in the short time behavior of the system, so we focus on the non-Markovian master equation (2.64). For times longer than the reservoir correlation time, however, the time-dependent coefficients reach their asymptotic Markovian value. We calculate, as an example, the Markovian value of the diffusion coefficient,

$$\begin{aligned}\Delta(t) &= 2\int_0^t ds \int_0^\infty d\omega\, J(\omega)\left[N(\omega)+\frac{1}{2}\right]\cos(\omega s)\cos(\omega_0 s) \qquad (2.99)\\ &= 2\int_0^\infty d\omega\, J(\omega)\left[N(\omega)+\frac{1}{2}\right]\frac{1}{2}\left[\frac{\sin[(\omega-\omega_0)t]}{\omega-\omega_0}+\frac{\sin[(\omega+\omega_0)t]}{\omega+\omega_0}\right].\end{aligned}$$

We can simplify this expression with the help of the Dirac delta function, defined as

$$\lim_{a\to 0}\frac{1}{a\pi}\frac{\sin x/a}{x/a}=\delta(x). \qquad (2.100)$$

If we define $t = 1/a$, we get

$$\lim_{t\to\infty} \frac{\sin tx}{x} = \pi\delta(x). \tag{2.101}$$

This can be used in Eq. (2.99) to obtain the Markovian value of $\Delta(t)$

$$\begin{aligned} \Delta_M &= \lim_{t\to\infty} \Delta(t) = \int_0^\infty d\omega\, J(\omega) 2 \left[N(\omega) + \frac{1}{2}\right] \frac{1}{2}\Big[\delta(\omega-\omega_0) + \delta(\omega+\omega_0)\Big] \\ &= \pi J(\omega_0)\left[N(\omega_0) + \frac{1}{2}\right]. \end{aligned} \tag{2.102}$$

In a similar manner we get the Markovian value for $\gamma(t)$,

$$\gamma_M = \frac{\pi}{2} J(\omega_0). \tag{2.103}$$

In short time scales the Markovian equations do not give correct dynamics because relevant memory effects are neglected. In longer time scales, however, the Markovian and non-Markovian dynamics coincide. Non-Markovian equations must be used, for example, in the context of atom lasers [21] or atoms decaying in photonic band gap materials [22].

Chapter 3

Modeling the interaction

3.1 Introduction

In the previous chapter we have modeled the interaction between system oscillator and the bosonic reservoir as a product between the position operators X and $\hat{x}_n$ for the system and environment operators, respectively. We have denoted with k_n the strength of interaction between the position operators of each individual environment oscillator and the system oscillator, see Eq. (2.17). We recall here the form of the interaction Hamiltonian

$$\alpha H_I = \alpha X \sum_n k_n \hat{x}_n, \tag{3.1}$$

where α is a dimensionless constant used to measure the overall strength of interaction. The master equation (2.64) we derived was based on the weak coupling approximation, so we assumed α small enough for the perturbative approach to be valid. In the limit of a continuum of reservoir modes, the function describing the strength of interaction is called spectral distribution and it has already been shown to depend on the frequency of the reservoir oscillators in Eq. (2.46). In the following sections we will introduce different types of spectral densities corresponding to different types of reservoirs. Different physical contexts, e.g., solid state, quantum optics and photonic crystals, are characterized by different spectral distributions.

By plotting the behavior of the decay coefficients for different types of reservoirs we gain an understanding of the fundamental way in which interaction with the environment changes the state of the damped harmonic oscillator. This comparative study of decoherence for different types of spectral distributions tells us which physical context, being less affected by decoherence, is more suitable for realizing quantum devices. We will discuss the physical interpretation of the various spectral densities to be introduced and provide figures to aid the analysis of the decay coefficients that we will consider in chapter 4.

3.2 Spectral density and distribution

We indicate with $J(\omega)$ a generic spectral density, which depends on the frequency of the environment oscillators. For a 3D-electric field, e.g., the specific form of $J(\omega)$ was given in Eq. (2.46). We now introduce the spectral distribution $I(\omega)$ obtained from the spectral density by multiplying it with $[N(\omega) + 1/2]$:

$$I(\omega) = J(\omega)\left[N(\omega) + \frac{1}{2}\right], \tag{3.2}$$

where $N(\omega)$ is the Planck distribution given in Eq. (2.37). This quantity tells us how the energy is distributed between the different modes of oscillation of the reservoir. The spectral distribution depends on the temperature of the reservoir through the Planck distribution $N(\omega)$. We can write the Planck term in Eq. (3.2) as

$$N(\omega) + \frac{1}{2} \equiv \coth\left(\frac{\omega}{2k_bT}\right). \tag{3.3}$$

By expanding this expression into Taylor series, we find that, for high temperatures T,

$$\coth\left(\frac{\omega}{2k_bT}\right) \approx \frac{2k_BT}{\omega}. \tag{3.4}$$

On the other hand, at zero temperature $N(\omega) = 0$, hence the thermal factor becomes simply $N(\omega) + \frac{1}{2} = \frac{1}{2}$. Therefore we get different approximated expression for

the spectral distributions (or spectra, for short) in the high temperature and zero temperature cases, namely,

$$I(\omega) = \frac{2k_BTJ(\omega)}{\omega} \quad \text{(high temperatures)} \tag{3.5}$$

$$I(\omega) = \frac{J(\omega)}{2} \quad \text{(zero temperature)}. \tag{3.6}$$

In this thesis, we focus on these two temperature regimes.

3.3 Different types of Ohmic spectral densities

Different physical contexts are characterized by different forms of environmental spectra, which in turn affect directly how fast the system decays. In quantum information devices the time it takes for the state of the system to decohere or decay, determines the available computational time. By using artificial engineered reservoirs as the environment of a qubit, researchers can manipulate the time available before the quantum state deteriorates. The motivation for studying different types of spectra stems partly from this objective. From a purely theoretical point of view this study gives us the tools to deepen our understanding of the underlying microscopic physical processes.

Thermal noise is characterized by a flat spectrum, while structured reservoirs are often encountered in solid state physics, e.g., in Josephson junctions [23], or when the density of reservoir modes is modified as, e.g., in photonic crystals [24]. By comparing different spectra we aim to chart the behavior of dissipation in the QBM model in different physical contexts. In this section we briefly examine three different paradigmatic spectra that are used later to evaluate numerically the decay and dissipation rates. It is useful to look at the differences in the spectral densities considered in order to understand the behavior of the decay dynamics. In this thesis a comparative study is conducted by taking into account reservoir spectral densities of the following form

$$J(\omega) = \alpha^2(\omega_{ph})^{1-s}\omega^s, \tag{3.7}$$

where we have included the dimensionless coupling constant α in the definition of $J(\omega)$, and where ω_{ph} is a reference frequency added to ensure that the spectral density has the unit of frequency. Here s is a variable and we will focus our attention to the cases where $s = 1/2, 1$ and 3. These are examples of the so called sub Ohmic, Ohmic and super Ohmic spectral distributions, respectively.

3.3.1 Ohmic case

The Ohmic spectral density corresponds to the choice $s = 1$. In this case

$$J(\omega) = \alpha^2 \omega. \tag{3.8}$$

This type of spectrum is one of the most common in the literature of open quantum systems. The Ohmic spectrum gives, for QBM, a friction-like force that is proportional to velocity. The Ohmic spectrum can be used, e.g., to describe charged interstitials (conductive electrons) in metals [20].

3.3.2 Super Ohmic case

The super Ohmic case corresponds to $s > 1$. Here we investigate $s = 3$, so the spectral density is given by

$$J(\omega) = \alpha^2 \frac{\omega^3}{\omega_{ph}^2}. \tag{3.9}$$

This form of spectral density corresponds, e.g., to a phonon bath in one or three dimensions, depending on the symmetry properties of the strain field [20]. It is also possible to show that this type of environment can be used in describing the effect of the interaction between a charged particle and its own electromagnetic field [25]. Also, the spectral distribution for the 3D-electric field given in Eq. (2.46) was exactly of this form.

3.3.3 Sub Ohmic case

Sub Ohmic case, with s=1/2, has the following spectrum

$$J(\omega) = \alpha^2 \sqrt{\omega_{ph}\omega}. \tag{3.10}$$

This type of noise may occur in some solid state devices and, in the high T case, is similar to the "1/f noise" in Josephson junctions [26].

3.4 Cutoff function

The spectral densities given above may lead to unphysical behavior since as ω grows, the spectral density increases without a limit, yielding divergence of certain physical quantities, such as momentum dispersion [20]. Physical spectral densities must fall off in the limit $\omega \to \infty$. To eliminate these divergencies one typically introduces a cutoff function ensuring that $J(\omega)$ goes to zero in the limit of infinitely high frequencies. It is reasonable to expect that the form of the cutoff function does not play a major role in the dissipative dynamics of the system at least as long as the cutoff is sufficiently far from the frequency of the system oscillator [20]. An example of the effect that different cutoffs have on the dynamics of the decay coefficient $\Delta(t)$ is demonstrated in Fig. 3.1 for three different cutoff functions. In particular we consider the commonly used Lorentz and exponential cutoff functions and the step function. The cutoff frequency ω_c appearing in the cutoff functions characterizes the duration of the system+reservoir correlations. Indeed the reservoir correlation time τ_R can be defined as $\tau_R = 1/\omega_c$ [29].

Lorentzian cutoff

By multiplying a Lorentzian cutoff function (sometimes called the Lorentz-Drude cutoff) with the spectral distribution given in (3.7), we obtain

$$J(\omega) = \alpha^2 (\omega_{ph})^{1-s} \omega^s \frac{\omega_c^2}{\omega_c^2 + \omega^2}. \tag{3.11}$$

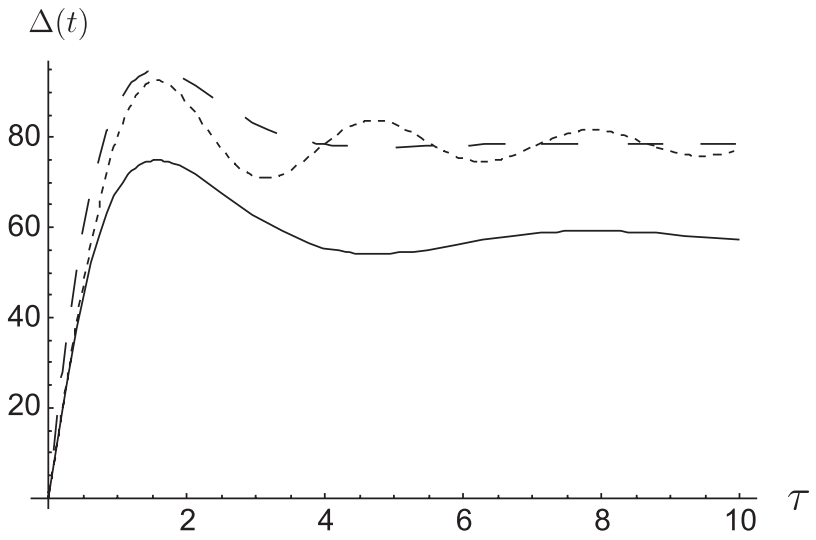

Figure 3.1: The main features of $\Delta(t)$ in the high temperature regime do not depend significantly on the choice of the cutoff function. The cutoff functions corresponding to the curves from top to bottom are the step function (dotted line), exponential (solid line) and Lorentzian (dashed line). In this figure we have set $\omega_c = \omega_0$.

Exponential cutoff

The spectral density with exponential cutoff is given by

$$J(\omega) = \alpha^2(\omega_{ph})^{1-s}\omega^s e^{-\omega/\omega_c}. \tag{3.12}$$

Step function

With a step function as the cutoff, the spectral distribution reads

$$J(\omega) = \alpha^2(\omega_{ph})^{1-s}\omega^s S(x), \tag{3.13}$$

where the step function is defined as

$$S(x) = \begin{cases} 1, & \text{if } x < \omega_c; \\ 0, & \text{if } x \geq \omega_c. \end{cases} \tag{3.14}$$

In the following we will focus on the exponential cutoff, because it turns out to be the most convenient for the calculations.

3.5 Parameter r

A relevant parameter in the description of the behaviour of the QBM model is

$$r = \frac{\omega_c}{\omega_0}, \tag{3.15}$$

i.e., the ratio between the cutoff frequency ω_c and the frequency of the system oscillator ω_0. This coefficient tells us whether our system is on resonance with the environment spectrum, or out of resonance. If $r \ll 1$, then $\omega_c \ll \omega_0$, which means that the system oscillates at a frequency much higher than the value of the cutoff frequency. In this case the system experiences quite a small effective coupling with the reservoir. This is the off resonant case. If $r \gg 1$, then $\omega_c \gg \omega_0$ and the system oscillator has a frequency ω_0 that lies within the most strongly coupled modes of the reservoir. In this case we say that the system is on resonance with the reservoir. At $r = 1$, ω_c is the same as ω_0, which indicates a somewhat intermediate situation compared to the two previous one. In this thesis we will focus on three exemplary values of r, covering the off resonant, resonant and intermediate regimes.

3.6 Plots of distribution functions

In the plots of the distribution functions for the sub Ohmic, Ohmic and super Ohmic reservoirs we have set $\omega_{ph} = \omega_c$.

The high temperature case

From Eqs. (3.2) and (3.7) it can be seen that for high temperatures we have

$$I(\omega) = \alpha^2(\omega_c)^{1-s}\omega^s \frac{2k_BT}{\omega} e^{-\omega/\omega_c}. \tag{3.16}$$

Our intention is to express this spectral distribution in a form that includes only fixed constants and one variable frequency $\bar{\omega}$, i.e., we want to have an expression of the type $I(\omega_0, r, \alpha, \bar{N}(\omega_0), \bar{\omega})$, where $\bar{N}(\omega_0) = N(\omega_0) + 1/2$. By defining

$$\bar{\omega} = \frac{\omega}{\omega_0}, \tag{3.17}$$

we obtain

$$I(\bar{\omega}) = 2\alpha^2 \bar{N}(\omega_0)\omega_0 \left(\frac{\bar{\omega}}{r}\right)^{s-1} e^{-\bar{\omega}/r}. \tag{3.18}$$

In the figures we plot the dimensionless quantity

$$\bar{I}(\bar{\omega}) = \frac{I(\bar{\omega})}{2\alpha^2 \bar{N}(\omega_0)\omega_0}. \tag{3.19}$$

The spectral densities for all three spectra are plotted in Fig. 3.2 for three different values of r. For better understanding the results presented in the following chapter it is useful to observe where the frequency of the oscillator ω_0 is located and how the strength of coupling, i.e., the value of $\bar{I}(\bar{\omega})$, experienced by the oscillator varies as we change the parameters of the reservoir, i.e., r, and the structure of the reservoir. This will explain indeed the differences in the decay dynamics of the QBM for different environments.

We can see from Eq. (3.17) that when $\omega = \omega_0$, we have $\bar{\omega} = 1$. This means that the frequency of QBM in harmonic potential, marked with solid red line, is located at $\bar{\omega} = 1$ in all the graphics in Fig. 3.2. The cutoff frequency, marked with a dotted black line, is defined with respect to the system frequency as $\omega_c = r\omega_0$.

The zero temperature case

At zero temperature the spectral density with exponential cutoff is

$$I(\omega) = \frac{J(\omega)}{2} = \frac{\alpha^2}{2}(\omega_c)^{1-s}\omega^s e^{-\omega/\omega_c}. \tag{3.20}$$

For plotting purposes we manipulate this expression in a similar manner as in the high temperature case, and get

$$I(\bar{\omega}) = \frac{\alpha^2}{2}\left(\frac{\bar{\omega}}{r}\right)^{s-1} \bar{\omega}\omega_0 e^{-\bar{\omega}/r}. \tag{3.21}$$

In the figures we plot

$$\bar{I}(\bar{\omega}) = \frac{2I(\bar{\omega})}{\alpha^2\omega_0}. \tag{3.22}$$

The plots of this expression are shown in Fig. 3.3.

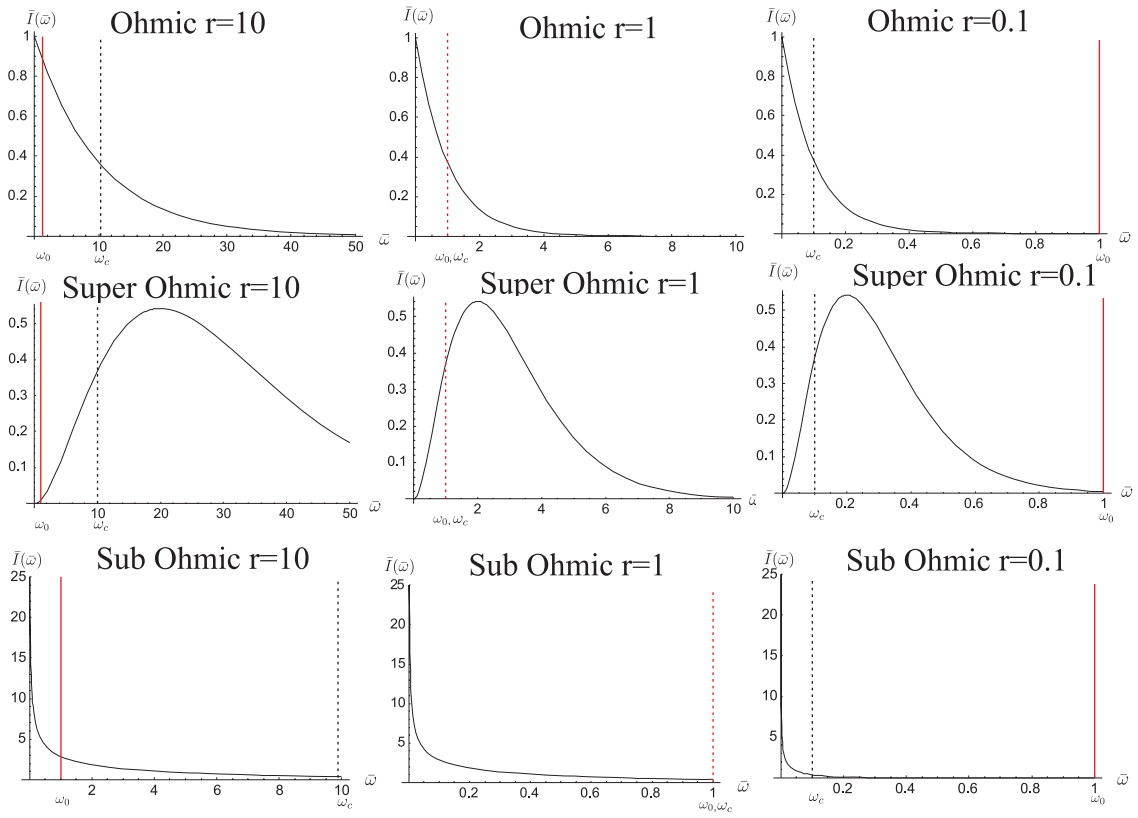

Figure 3.2: Spectral distributions $\bar{I}(\bar{\omega}) = I(\bar{\omega})/(2\alpha^2 \bar{N}(\omega_0)\omega_0)$ for Ohmic, super Ohmic and sub Ohmic cases at high temperatures. The frequency of the system oscillator is always located at $\bar{\omega} = 1$. Different values of r correspond to different positioning of the oscillator frequency ω_0 with respect to the cutoff frequency ω_c, i.e., $r = \omega_c/\omega_0$. In sub Ohmic case, the spectrum diverges for $\bar{\omega} = 0$.

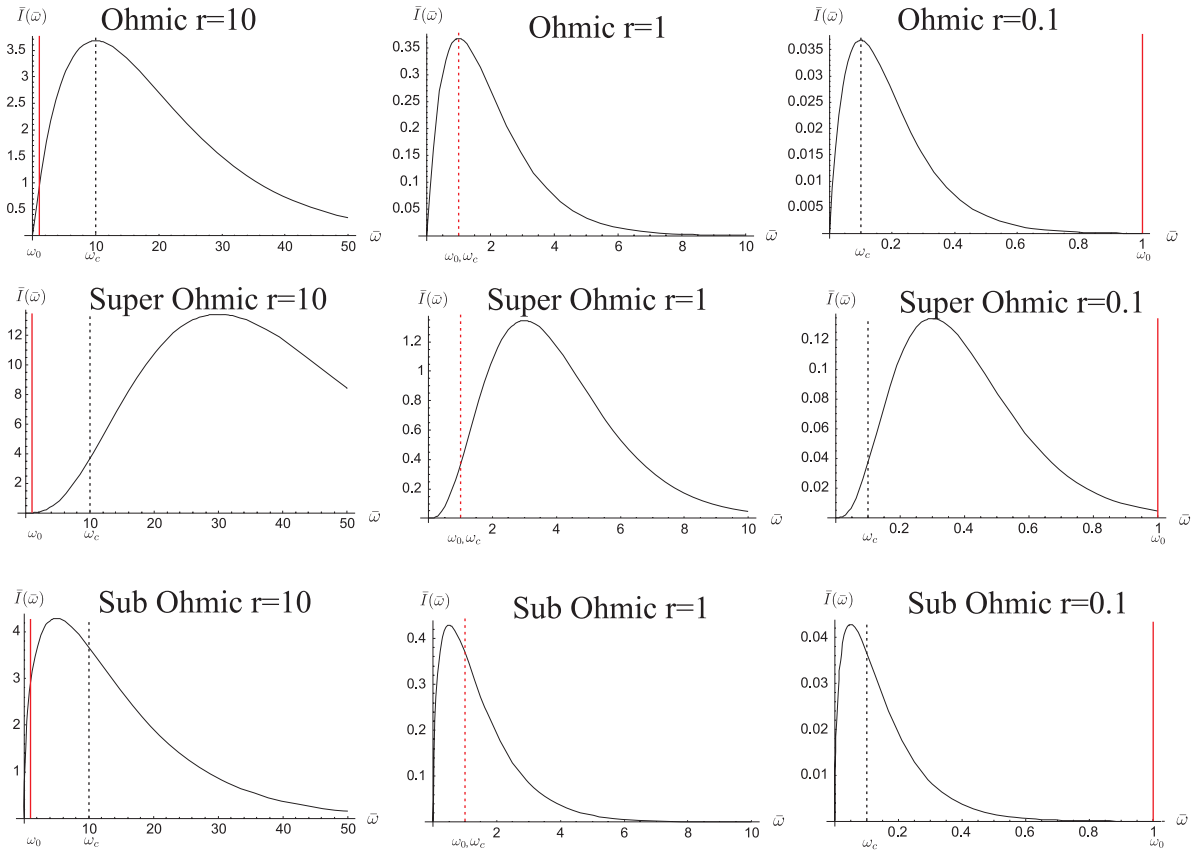

Figure 3.3: Spectral distributions $\bar{I}(\bar{\omega}) = 2I(\bar{\omega})/(\alpha^2\omega_0)$ for Ohmic, super Ohmic and sub Ohmic reservoirs at zero temperature. The frequency of the system oscillator is depicted as a solid red line and it is always positioned at $\bar{\omega} = 1$. We consider three different exemplary values of $r = \omega_c/\omega_0$.

Chapter 4

Decay rates

4.1 Introduction

In this chapter we will examine the dynamics of the time-dependent coefficients $[\Delta(t) \pm \gamma(t)]/2$, where $\Delta(t)$ and $\gamma(t)$ are the diffusion and damping coefficients defined in Eqs. (2.65) and (2.66), respectively. These coefficients represent the relaxation rates for the decay channels of the QBM model [5]. In the Fock state basis the decay channels are associated with the transition $|n\rangle \to |n+1\rangle$ given by the operator $a^\dagger$, and the transition $|n\rangle \to |n-1\rangle$ given by the operator a. These transitions happening via the decay channels destroy the quantum coherence of initial quantum superpositions. The rates at which these processes occur are given by the coefficients $[\Delta(t) \pm \gamma(t)]/2$, i.e., the decay rates. The transition up channel, corresponding to the heating process, is associated with the decay rate

$$\frac{\Delta(t) - \gamma(t)}{2} \qquad (\text{transition up}), \tag{4.1}$$

while the transition down channel corresponding to the cooling process, is associated with the dacay rate

$$\frac{\Delta(t) + \gamma(t)}{2} \qquad (\text{transition down}). \tag{4.2}$$

From the definition of $\Delta(t)$ in Eq. (2.65) one sees immediately that the rate at which the decay occurs depends on the type of reservoir through the spectral density $J(\omega)$. We study the decay rates in three different reservoirs and in both the zero and the high temperature reservoirs. The decay rates always start from zero and after some time they reach their constant Markovian value, which is always non-negative. In some cases the rates may acquire temporarily negative values. It has been shown that, when the time-dependent coefficients attain negative values, the corresponding decay channel operates in a reverse way, i.e., the down channel actually induces heating and vice versa [27].

4.2 High temperature case

By looking at $\Delta(t)$ and $\gamma(t)$ given in Eq. (2.65) and (2.66) we notice that only the $\Delta(t)$ term depends on the Planck distribution, which for high temperatures is approximated by $2k_BT/\omega$. Therefore, for high temperatures and for times much smaller than the thermalization time τ_{th}, $\Delta(t) \gg \gamma(t)$. Under these conditions, the two decay channels operate at the same rate, namely, $\Delta(t)/2$. By plugging in the spectral density given in Eq. (3.16) into Eq. (2.65), the following expression is obtained:

$$\Delta(t) = 4\alpha^2 k_B T \int_0^t dt' \int_0^\infty d\omega \left(\frac{\omega}{\omega_c}\right)^{s-1} e^{-\omega/\omega_c} \cos(\omega t') \cos(\omega_0 t'). \tag{4.3}$$

The integral with respect to ω can be solved analytically. The remaining integration with respect to time t', however, must be calculated numerically. We have plotted $\Delta(t)$ for the three different reservoirs given in Eqs. (3.8), (3.9) and (3.10) and with three different values of the parameter r. The results we obtained are shown in Fig. 4.1. In the plots we use dimensionless time τ, with $\tau = \omega_c t$. The front factor of $\Delta(t)$ is set to

$$4\alpha^2 k_B T = 100. \tag{4.4}$$

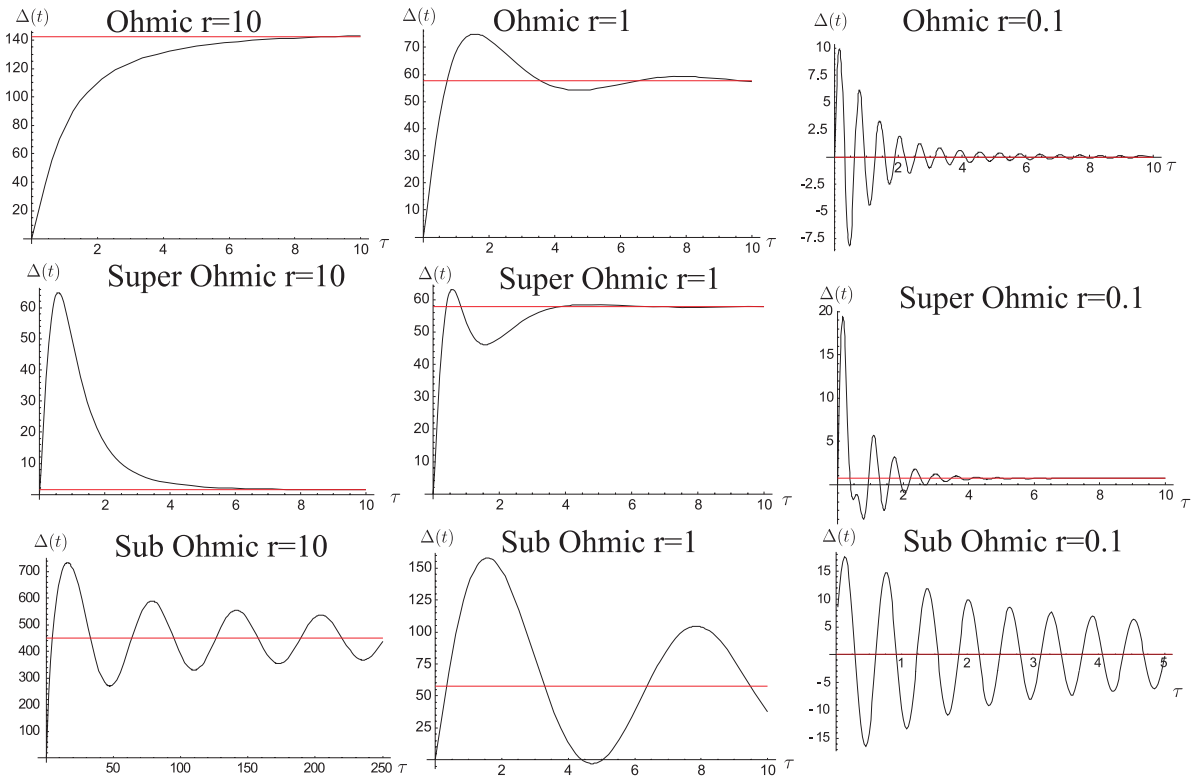

Figure 4.1: Decay rate $\Delta(t)$ for high temperatures. The red horizontal line depicts the Markovian value $\Delta_M = \lim_{t\to\infty} \Delta(t)$.

We have included in the plots the Markovian value of $\Delta(t)$, which is obtained from Eq. (2.102) by simply plugging in the spectral distribution for high temperatures given by Eq. (3.16). The Markovian value is

$$\Delta_M(t) = \frac{100\pi}{4}\left(\frac{1}{r}\right)^{s-1} e^{-1/r}, \tag{4.5}$$

and it is denoted by a solid red line in Fig. 4.1. When analyzing the results it is important to keep in mind Fig. 3.2 picturing the spectral densities. We now look at the dynamics of $\Delta(t)$ for different values of r and different reservoir spectra. Let us start by comparing changes in $\Delta(t)$ arising from variations of the values of the parameter r. When moving from $r \ll 1$ to $r \gg 1$, we notice two distinct features in the dynamics of $\Delta(t)$ common to all of the reservoir spectra.

The first common feature is that while oscillations in $\Delta(t)$ may still be present,

$\Delta(t)$ becomes always positive. In fact, $\Delta(t) < 0$ for certain time intervals only when $r \ll 1$. This is important for understanding the dynamics of the heating function in the next chapter. By comparing this oscillatory behavior to the reservoir spectra in Fig. 3.2, we notice that the amplitude and the presence of oscillations itself arise from that part of the spectrum with $\omega < \omega_0$. In the sub Ohmic case the spectrum has a divergency point at $\omega = 0$, so a large part of the spectrum lies very near this point. This explains why the oscillations are always present in the sub Ohmic case, while in the other two reservoirs the oscillations are lost when r increases.

The second characteristic feature arising for $r \gg 1$ is the increase in the Markovian value of $\Delta(t)$. The only exception to this rule is the super Ohmic case with $r = 10$. Equation (2.102) shows that the Markovian value of $\Delta(t)$ is directly proportional to the strength of the coupling at the oscillator location, i.e., $\Delta_M \propto I(\omega_0)$, as one can also see by comparing Figs. 3.2 and 4.1. This explains the deviate behavior of the super Ohmic $r = 10$ case: the value of $I(\omega_0)$ for $r = 10$ is simply smaller than in the $r = 1$ or $r = 0.1$ cases.

In order to understand how different types of reservoirs affect the dynamics, we fix the value of r. In the $r = 0.1$ case, oscillations and negative values of $\Delta(t)$ appear for all of the reservoir types. As mentioned above, in the off resonant case, the low frequency part of the spectrum is dominant and thus oscillations are expected. In the super Ohmic and Ohmic cases these oscillations are damped more rapidly than in the sub Ohmic case. When $r = 1$, the sub Ohmic case oscillates with a large amplitude for a long time, while the other two cases exhibit almost identical dynamics with only a few rapidly damped oscillations. The Markovian values are practically the same in all three cases, which results from the fact that also $I(\omega_0)$ has almost the same value in all the cases. For $r = 10$, the sub Ohmic case exhibits oscillations that damp very slowly. The other two reservoirs show no oscillations at all, which is consistent with the fact that there is only a small amount of spectrum in the low frequency range. There is a strong initial "bump" in the super Ohmic case,

but in Ohmic case $\Delta(t)$ approaches the Markovian value monotonically. The bump in the super Ohmic case might be due to the fact that most of the spectrum is in the high frequency range. High frequencies contribute to the short time dynamics. These short time scale effects can have substantial impact on the non-Markovian dynamics of $\Delta(t)$. These effects might be responsible for the rapid increase in $\Delta(t)$ for short non-Markovian times in the super Ohmic case. For $t \gg \tau_c$, $\Delta(t)$ quickly decreases to its (smaller) Markovian value.

For quantum information purposes decoherence and dissipation are unwanted phenomena, and therefore the most preferable reservoir is the one that induces least amount of deteriorating effects on the qubit implemented, e.g., by a single trapped ion. Current quantum computing devices operate in time scales that are essentially Markovian. However, if we wish to reduce the harmful decoherence induced by the environment, we need to shorten the time needed to perform a logical operation in quantum computing devices. This leads to non-Markovian dynamics. In this case we have to take the short time dynamics of $\Delta(t)$ and $\gamma(t)$ into account. That is, when judging which of the reservoirs introduced in Section 3.3 causes least amount of dissipation/decoherence we need to evaluate the slope of the decay rate, not its Markovian value. More precisely, we have to first decide how long we need to protect a qubit from the effects of the environment and then determine which reservoir is the best, i.e., which reservoir has the smallest decay rate up to that point of time. The time scales in different reservoirs are not directly comparable in our figures, because they are plotted in units of ω_c and the choice of r affects the time scale as well.

4.3 Zero temperature case

For zero temperature the time-dependent coefficients in the master equation (2.64) take the following form

$$\Delta(t) = 2\alpha^2 \int_0^t dt' \int_0^\infty d\omega \, \frac{\omega_c}{2} \left(\frac{\omega}{\omega_c}\right)^s e^{-\omega/\omega_c} \cos(\omega t') \cos(\omega_0 t') \tag{4.6}$$

$$\gamma(t) = 2\alpha^2 \int_0^t dt' \int_0^\infty d\omega \, \frac{\omega_c}{2} \left(\frac{\omega}{\omega_c}\right)^s e^{-\omega/\omega_c} \sin(\omega t') \sin(\omega_0 t'). \tag{4.7}$$

In this case, contrary to the high temperature regime, $\Delta(t)$ and $\gamma(t)$ are of the same order of magnitude. The transition up and transition down channels are given by Eq. (4.1) and (4.2), respectively. Because the reservoir is at zero temperature, the transition up channel is expected to close for $\omega_c t \gg 1$, while the decay rate for transition down channel reaches eventually its positive Markovian value.

Since the reservoir is at zero temperature, it would seem plausible that no transitions up can occur because the reservoir is empty of energy. However, the interaction Hamiltonian (2.17) induces an oscillatory behavior in the coefficients $\Delta(t)$ and $\gamma(t)$ giving rise to a non-zero transition up rate. The interaction Hamiltonian gives us four terms characterizing the emission and absorption processes, namely, ab_n, $ab_n^\dagger$, $a^\dagger b_n$ and $a^\dagger b_n^\dagger$. The two terms in the middle correspond to real processes conserving the unperturbed energy, while the other two are known as the counter rotating terms. These terms describe the simultaneous creation or annihilation of a quantum of energy both in the system and in the reservoir oscillators. The energy required for such processes to occur comes from the system-reservoir coupling. A schematic figure of these processes is shown in Fig. 4.2. By combining these two counter rotating terms, we obtain a process that corresponds to energy conserving processes, as depicted in Fig. 4.3. It can be shown that at zero temperature the dynamics of the decay rate for the transitions up originate from these counter rotating terms [11]. The oscillations in $\Delta(t)$ and $\gamma(t)$ have also a role in the dynamics of the energy of the harmonic oscillator, as we will see in the next chapter. In the Markovian approximation the counter rotating terms are neglected and the transition up rate,

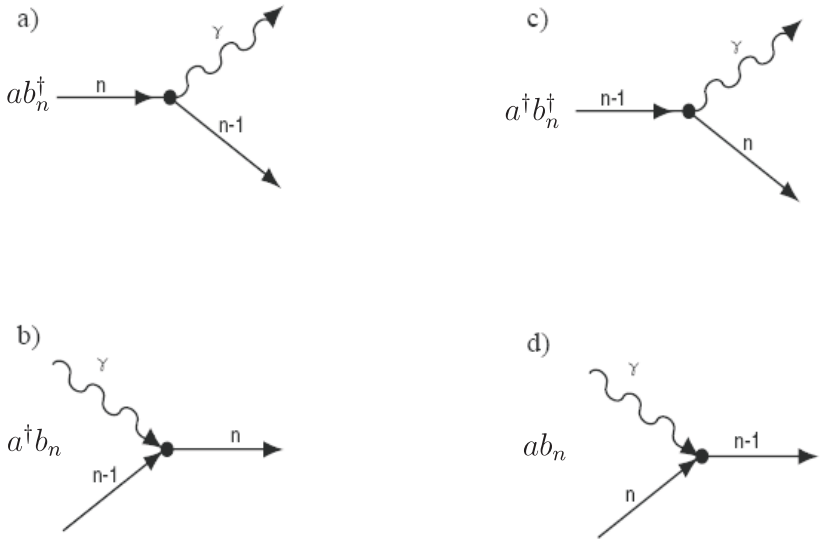

Figure 4.2: The four terms in the interaction Hamiltonian. Here γ is one quantum of energy and n is the number state in the Fock state basis. The terms a) and b) correspond to real processes, while the c) and d) terms are virtual processes that do not conserve the unperturbed energy. Figure is taken from [11].

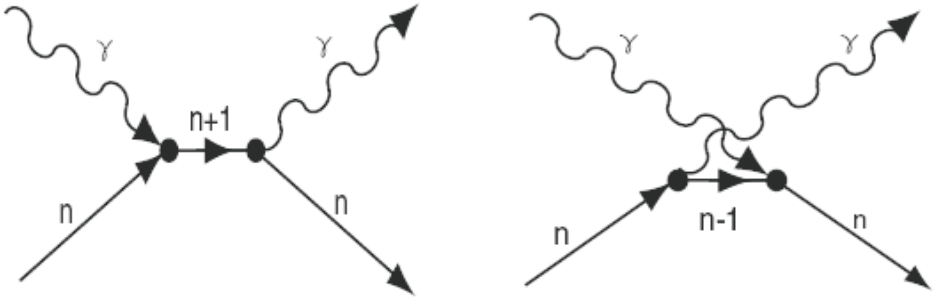

Figure 4.3: By combining processes a)+b) and c)+d) in Fig. 4.2 we obtain two energy conserving processes. In the figure γ is one quantum of energy and n is the number state in the Fock state basis. The process on the left is a real process, while process on the right originates from two virtual processes that conserve energy when combined in this way. Figure is taken from [11].

in the case of zero temperature reservoir, is always zero.

With the help of Eqs. (2.102) and (2.103) we can calculate the Markovian value of the decay rate for downward transition

$$\lim_{t\to\infty} \frac{\Delta(t)+\gamma(t)}{2} = \frac{\pi}{2} J(\omega_0), \tag{4.8}$$

while the Markovian value for the decay rate for upward transition is, as expected,

$$\lim_{t\to\infty} \frac{\Delta(t)-\gamma(t)}{2} = 0. \tag{4.9}$$

The results we obtained for the decay rates are shown in Figs. 4.4, 4.5 and 4.6 for the $r = 10$, 1 and 0.1 cases, respectively.

We observe that the intervals of time at which the transition rates $\Delta(t) \pm \gamma(t)$ attain negative values diminishes when r goes from $r \ll 1$ to $r \gg 1$, just like in the high temperature case. The reason is once more found in the structure of the spectra shown in Fig. 3.3, i.e., a large part of the spectrum lies in the low frequency range when $r \ll 1$. It is worth noticing that $\Delta(t) - \gamma(t)$, for $r = 10$ and in the super Ohmic case, still oscillates between negative and positive values before reaching its final zero value. While practically no spectrum lies in the low frequency range in this case, an explanation to this anomaly exists. For certain time intervals, indeed, $\Delta(t) < \gamma(t)$, and therefore $\Delta(t) - \gamma(t)$ is negative even if the low frequency part of the reservoir spectrum does not contribute significantly.

One evident feature in the plots is that the super Ohmic spectrum seems to be inducing the steepest decay rates for all values of r. One way to interpret this is to remember that super Ohmic spectrum is used to model three dimensional environments. In a way, due to the higher dimensionality, the system is more strongly coupled in the super Ohmic case than in the Ohmic and sub Ohmic cases. This leads to faster dissipation compared to the other environments. An interesting aspect worth mentioning in the plots of the decay rates is visible in super Ohmic case with $r = 10$, depicted in Fig. 4.6 as the dotted line. We observe that the transition down channel nearly closes when $\bar{\omega} \approx 3$, and around the same time the transition up

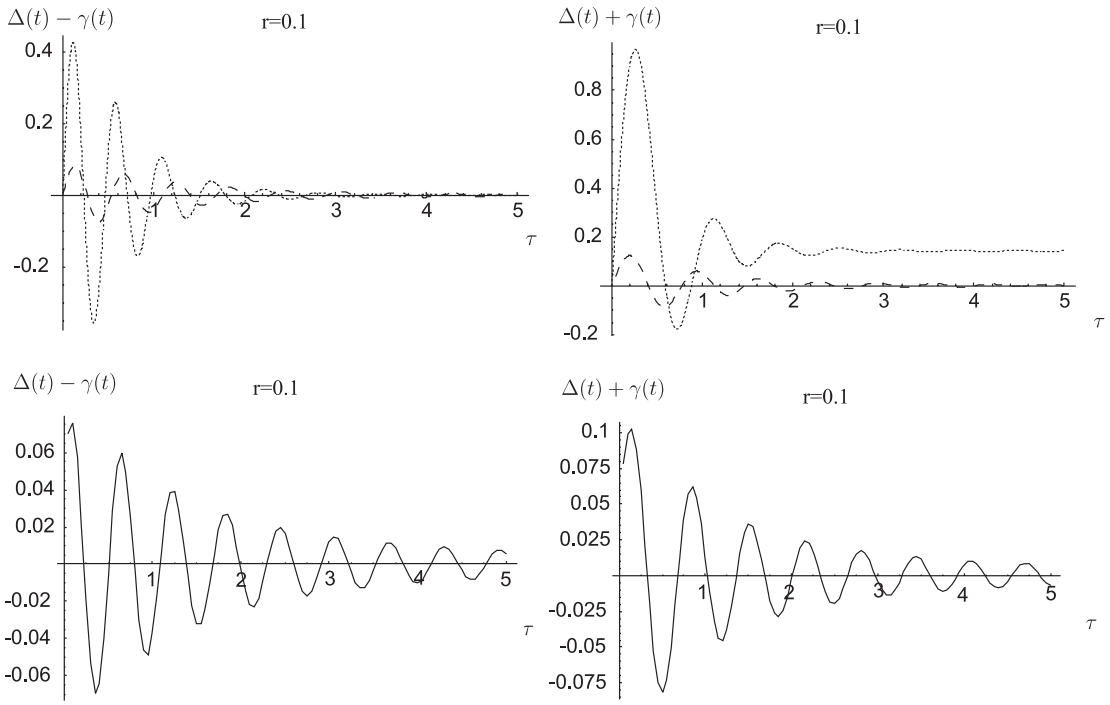

Figure 4.4: The decay rates at zero temperature in the off resonant $r = 0.1$ case. Ohmic (dashed line) and super Ohmic (dotted line) cases are shown in the upper plots. The sub Ohmic case (solid line) is plotted separately. The figures on the left show the transition up rates, while the figures on the right show the transition down rates.

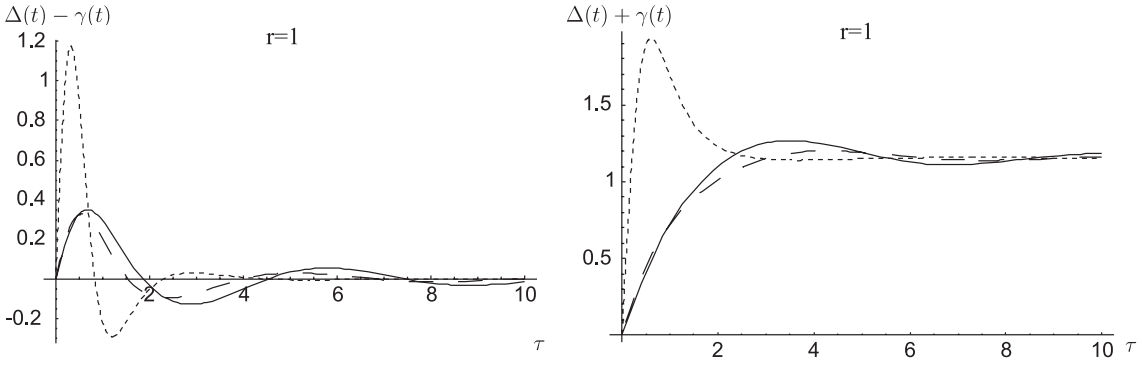

Figure 4.5: The decay rates for parameter $r = 1$ at zero temperature for sub Ohmic (solid line), Ohmic (dashed line) and super Ohmic (dotted line) cases. The figure on the left shows the transition up rates, while the figure on the right shows the transition down rates.

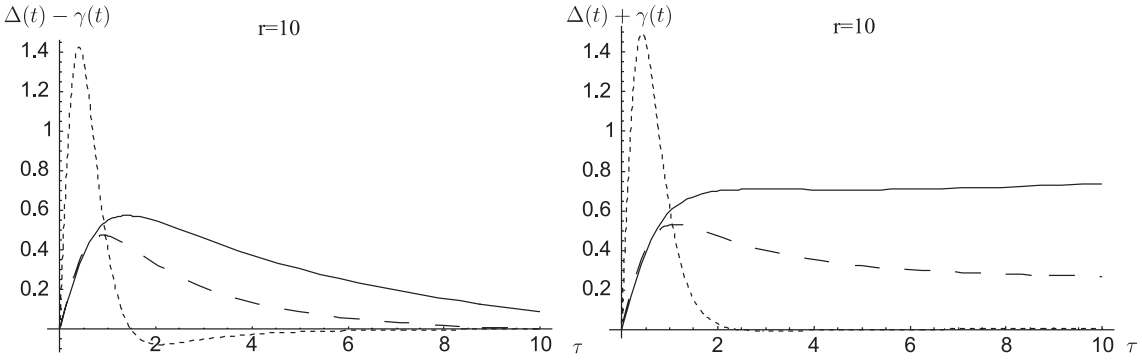

Figure 4.6: The decay rates for parameter $r = 10$ at zero temperature for sub Ohmic (solid line), Ohmic (dashed line) and super Ohmic (dotted line) cases. The figure on the left shows the transition up rates, while the figure on the right shows the transition down rates.

rate becomes negative and tends to zero from the negative side. It has been proven in Ref. [27] that in correspondence to negative regions in $\Delta(t) \pm \gamma(t)$, reverse transitions restoring the previous quantum state occur. In view of these results one can argue that, in the case considered above, the up channel acts like a transition down channel. This implies that the thermalization is achieved via a reverted transition up channel, while the actual transition down channel is almost completely closed.

Chapter 5

Dissipation dynamics

In this chapter we consider the dissipation dynamics of the QBM in terms of the heating function $\langle n(t)\rangle$, which is defined as the mean number of excitations in the oscillator, where n is the number operator $a^\dagger a$. The heating function is closely related to the energy of the quantum harmonic oscillator defined as

$$\langle E\rangle = \hbar\omega_0 \left(\langle n(t)\rangle + \frac{1}{2}\right). \tag{5.1}$$

Since the system oscillator is interacting with a thermal reservoir its energy will eventually approach the thermal value $k_B T$, with T the reservoir temperature. We will now look at the heating function dynamics for time scales much shorter than the thermalization time.

5.1 Heating function

We obtain an expression for the heating function $\langle n(t)\rangle$ by using the secularly approximated quantum characteristic function of QBM given in Eq. (2.97), with the help of the relations given by Eqs. (2.69) and (2.70). As was stated in Section 2.4, the secular approximation does not affect the dynamics of the mean energy of a quantum harmonic oscillator. Therefore, we obtain the following exact expression

for the heating function

$$\langle n(t)\rangle = e^{-\Gamma(t)}\langle n(0)\rangle + \frac{1}{2}\left[e^{-\Gamma(t)} - 1\right] + \Delta_\Gamma(t), \tag{5.2}$$

where $\Gamma(t)$ and $\Delta_\Gamma(t)$ are given by Eqs. (2.80) and (2.98), respectively. We will focus on the case where the initial state of the oscillator is the ground state, i.e., $\langle n(0)\rangle = 0$. We study the heating function dynamics looking at the short and long time scales separately. Long time refers to times much longer than the reservoir correlation time τ_R corresponding to the Markovian dynamics.

5.1.1 Heating function in long time scales

In the long time limit, we can replace the values of $\Delta(t)$ and $\gamma(t)$ appearing in the terms $\Gamma(t)$ and $\Delta_\Gamma(t)$ of Eq. (5.2) with their constant Markovian values Δ_M and γ_M. The heating function in this case takes the form

$$\langle n(t)\rangle = N(\omega_0)\left(1 - e^{-\Gamma t}\right), \tag{5.3}$$

where $\Gamma = 2\gamma_M$. From the above equation we see that when the system thermalizes, we obtain $\langle n(t)\rangle_{t\to\infty} = N(\omega_0)$. To investigate how the system oscillator approaches thermalization we study the function

$$\frac{\langle n(t)\rangle}{N(\omega_0)} = 1 - \exp\left[-2\pi\alpha^2\left(\frac{1}{r}\right)^{s-1} e^{-1/r}\tau\right], \tag{5.4}$$

where we have used the expression for γ_M obtained by combining Eqs. (2.103) and (3.7), with an exponential cutoff, with $\tau = \omega_0 t$. For simplicity, we have also set $2\pi\alpha^2 = 1$. Now we can directly compare the thermalization times for different reservoirs. The results are shown in Figs. 5.1-5.4. Because of a difference in the scale, the off resonant case with $r = 0.1$ is shown separately in Fig. 5.4. We considered here the high temperature case, so the corresponding environmental spectra are shown in Fig. 3.2. As we can see by comparing the graphics of the heating function to the reservoir spectra the time it takes to thermalize in a given environment depends

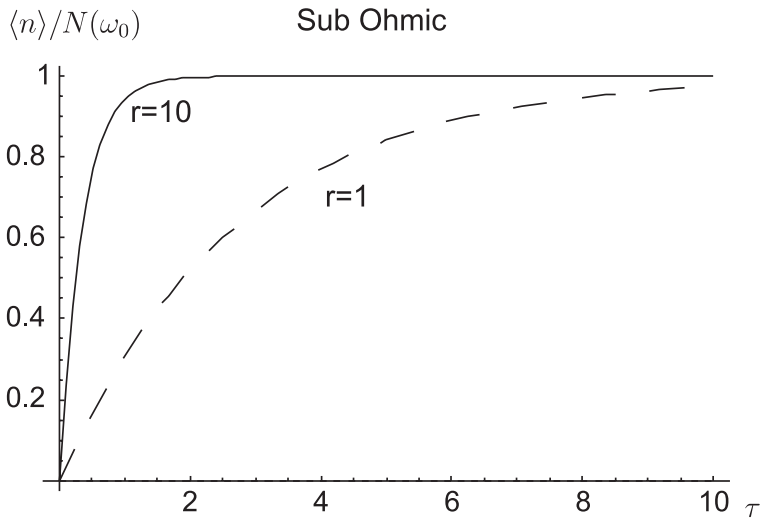

Figure 5.1: Heating function in the sub Ohmic case for long times. The resonant case corresponding to $r = 10$ thermalizes first because the coupling is the strongest.

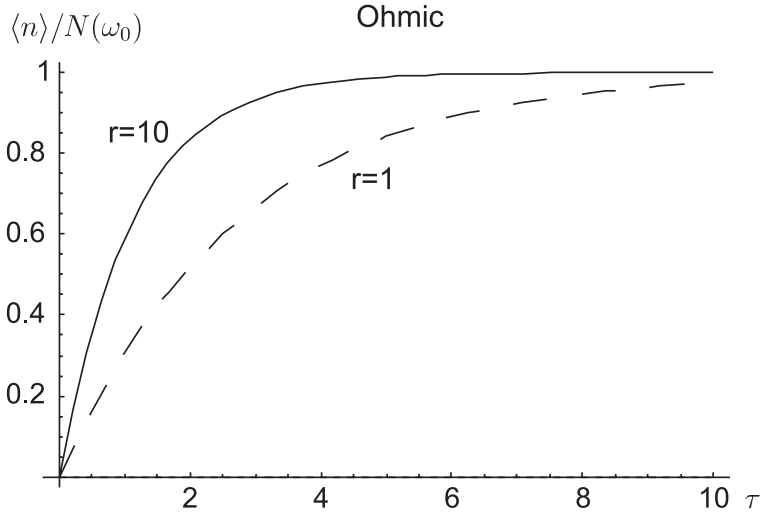

Figure 5.2: Heating function in the Ohmic case for long times.

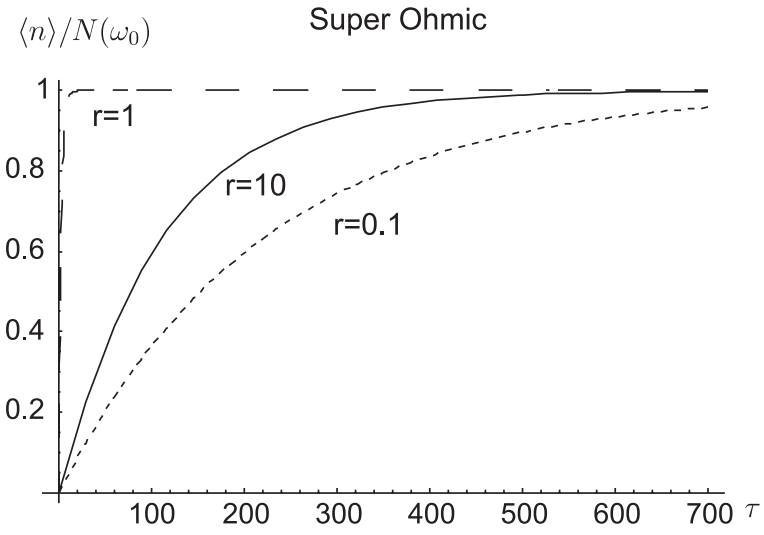

Figure 5.3: Heating function in the super Ohmic case for long times. Now $r = 1$ case thermalizes the fastest and even the $r = 0.1$ case shows thermalization time that is of the same order of magnitude as for the other two cases.

on the strength of the coupling at the oscillator location, i.e., on the value $I(\omega_0)$. Thus, in general, the more detuned the reservoir is, the slower is the thermalization of the system. The off resonant case with $r = 0.1$ is plotted in Fig. 5.4 in order to see more clearly what actually happens. From this figure it can be observed that due to the structure of the reservoir spectra, the super Ohmic case thermalizes at the fastest rate, while now it is the Ohmic case, that heats up at the slowest rate, meaning that the coupling is weaker in the Ohmic than in the sub Ohmic case. This can be confirmed by looking at Fig. 3.2.

5.1.2 Non-Markovian dynamics of the heating function

We now focus on the dissipation dynamics of the QBM for times much shorter than the thermalization time τ_{th} and for the initial ground state. Under these conditions, Eq. (5.2) can be approximated as

$$\langle n(t)\rangle = \int_0^t \left[\Delta(t_1) - \gamma(t_1)\right] dt_1. \tag{5.5}$$

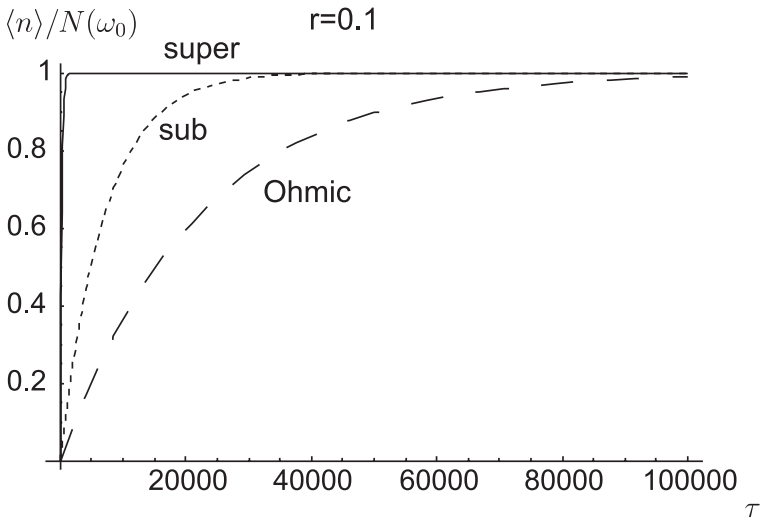

Figure 5.4: Long time heating function for the off resonant case. Here it is clearly visible that different reservoirs cause thermalization to occur at different times even in the off resonant case, which was not clearly visible in the previous graphics.

The reason why $\langle n(t)\rangle$ in the above equation only depends on the transition up channel, characterized by $\Delta(t) - \gamma(t)$, stems from our choice of the initial condition. For times $t \ll \tau_{th}$, indeed, the probability that the system absorbs one quantum of energy from the environment, is much higher than the opposite process, i.e., the emission of a quantum of energy from the system to the environment.

For high temperature reservoirs, Eq. 5.5 can be approximated as follows

$$\langle n(t)\rangle = \int_0^t \Delta(t_1)\, dt_1. \tag{5.6}$$

It is clear that the sign of $\Delta(t)$ determines whether the dynamics of the heating function exhibit monotonic or oscillatory behavior. The plots of the heating function for high temperature and for $t \ll t_{th}$, are given in Figs. 5.5 - 5.7.

It has been shown in Ref. [13] that, for an Ohmic spectral density, the main features of the dynamics of $\langle n(t)\rangle$ may be grouped into two types of behavior and that there exists a connection between these main features and the spectral distribution. The heating function, indeed, can either grow monotonically or present small amplitude oscillations superposed to the monotonic growth. In Ref. [13] it

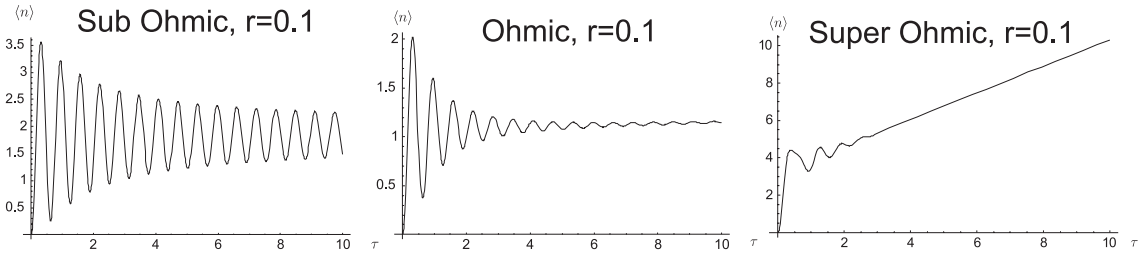

Figure 5.5: Short time dynamics of the heating function $\langle n(t)\rangle$ for different reservoirs. Here depicted at $r = 0.1$, i.e., when the system is off resonant. Plots are given in dimensionless time $\tau = \omega_c t$.

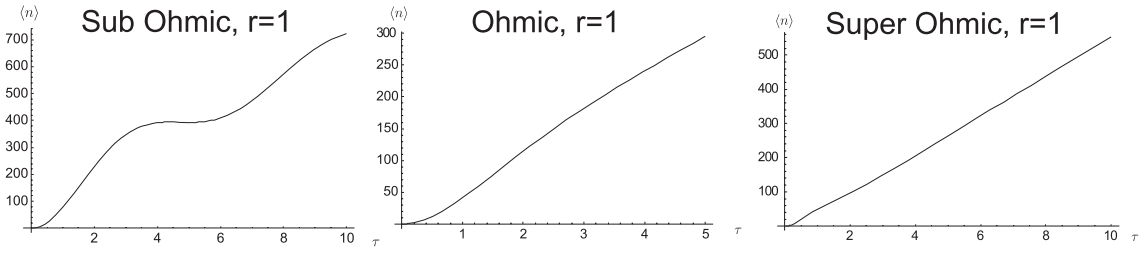

Figure 5.6: Short time dynamics of the heating function $\langle n(t)\rangle$ for different reservoirs. Here depicted at $r = 1$. Plots are given in dimensionless time $\tau = \omega_c t$.

was shown that the oscillatory dynamics originate from the low frequency part of the spectrum, while the monotonic growth is related to the resonant part of the spectrum, i.e., essentially, to the value of $I(\omega_0)$. By comparing the plots in Figs. 5.5 - 5.7 and the high temperature spectra in Fig. 3.2 we see that, also for the different environmental spectra studied in this thesis, the dynamics can be explained with this division in mind. In the off resonant case, i.e., when $r \ll 1$ we see from Fig. 5.5 that oscillations are present in all the reservoirs, since nearly the whole spectrum lies in this case at low frequencies. In the Ohmic and sub Ohmic cases the heating function appears to reach some constant value, while in the super Ohmic case it keeps growing. This is due to the fact that in the super Ohmic $r = 0.1$ case, compared to the other two reservoirs, the strength of the coupling is greater at the oscillator location. In the $r = 1$ case, we see from Fig. 5.6 that there are

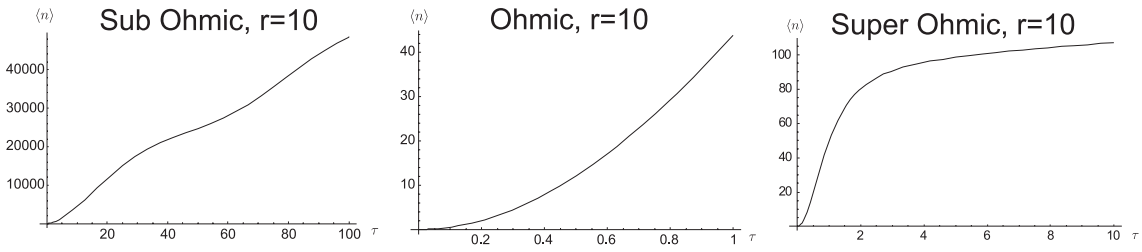

Figure 5.7: Short time dynamics of the heating function $\langle n(t)\rangle$ for different reservoirs. Here depicted at $r = 10$, i.e., when the system is off resonant. Plots are given in dimensionless time $\tau = \omega_c t$.

no oscillations. The heating function grows in a monotonic manner in all the cases. With the sub Ohmic reservoir there exists a level plateau in $I(\omega) \approx 5$, resulting from the fact that the oscillations in $\Delta(t)$ almost reach negative values. In the resonant case, i.e., when $r \gg 1$, the behavior of the heating function in the super Ohmic case differs qualitatively from the Ohmic and sub Ohmic dissipation. Namely, the heating function grows quickly first and then almost approaches a constant value, for $\tau > 10$, before reaching the Markovian regime. The slow increase of $\langle n(t)\rangle$ after the initial fast growth can be explained by the fact that $I(\omega_0)$ is extremely small, ≈ 0.01. The initial growth originates from the bump in the decay rate $\Delta(t)$ pictured in Fig. 4.1. When we integrate over this bump, $\langle n(t)\rangle$ grows rather rapidly but the growth is slowed down because the final value of the decay rate, Δ_M, is small.

The oscillations in the heating function tell us that in the thermalization process the system can give back to the reservoir some of the energy that has previously absorbed from it. In other words, the direction of the energy flow is reversed during the time periods in which the slope of $\langle n(t)\rangle$ is negative. These oscillations are a sign of the non-Markovian dynamics. Due to the finite reservoir memory the system recovers some of the information/energy "lost" in the reservoir.

When the system oscillator interacts with a zero temperature reservoir, for an initial ground state, the dynamics of the heating function are basically due to the finite, although small, system-reservoir coupling energy. The short time behavior of

$\langle n(t)\rangle$ at zero temperature can be obtained by plotting Eq. (5.5). To give an example of the dynamics, we have plotted this equation in Fig. 5.8 for an Ohmic reservoir. We see that oscillations are present when $r = 0.1$ and $r = 1$. This corresponds to the occurrence of temporarily negative values of $\Delta(t) - \gamma(t)$ depicted in Figs. 4.4-4.5. When the system thermalizes, the dynamics disappear as $\lim_{t\to\infty}\langle n(t)\rangle = 0$.

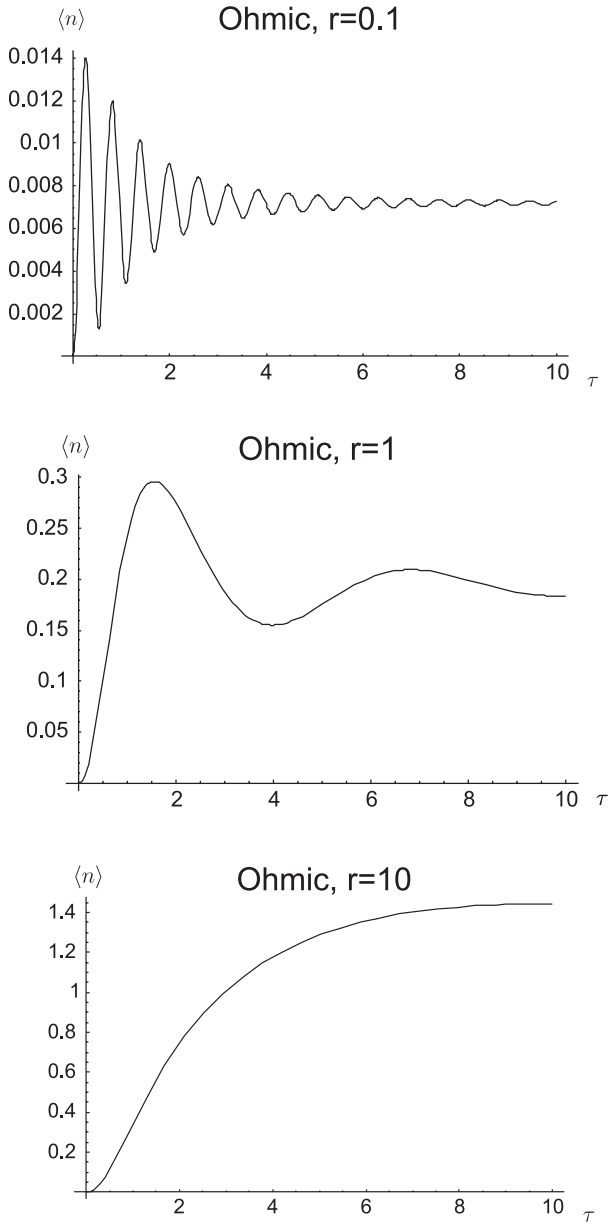

Figure 5.8: Short time dynamics of the heating function $\langle n(t)\rangle$ at zero temperature for the Ohmic reservoir. Plots are given in dimensionless time $\tau = \omega_c t$.

Chapter 6

Summary and conclusions

The purpose of this thesis was to investigate how the dynamics of an open quantum system depend on the structure of the reservoir. We considered the quantum Brownian motion model, in the specific case of a harmonic potential. Starting from a closed total system consisting of the system oscillator and a thermal reservoir, we derived a perturbative master equation for the open reduced system. An exact master equation was introduced for reference. The exact and the perturbative master equations are equivalent in the conditions we focus on, namely, in the weak coupling regime for certain classes of observables such as the heating function. We briefly reviewed the derivation of the exact solution of the exact master equation. This solution allows one to obtain an analytical expression for the heating function.

The master equation we consider is local in time and of Lindblad type. The non-Markovianity of the system is reflected in the presence of the time-dependent decay rates which entail all the information about decoherence and dissipation. We have considered different examples of environmental spectra, and we have evaluated the dynamics of the QBM both in zero and high temperatures.

For time scales much shorter than the thermalization time of the reduced system, the decay rates in the master equation exhibit characteristic non-Markovian features. We have seen that typical non-Markovian dynamics are characterized by oscillations

that result from the reservoir memory, as for the case of the heating function. We also investigated the relationship between the temporal behavior of the decay rates and the spectral structure of the reservoir. We noticed that when the system is off resonant with respect to the reservoir, the decay rates in both temperature regimes exhibit oscillations attaining temporarily negative values. In the resonant case, the decay rates are always positive for high temperatures. However, the sub Ohmic reservoir induced oscillations even in the resonant regime, while the Ohmic and super Ohmic reservoirs did not. We have also seen that the spectral distribution at the oscillator location affects the Markovian value of the decay rates, i.e., the stronger the coupling, the higher is the Markovian decay rate.

At zero temperature the decay rates for transitions up and down have different values, whereas in the high temperature approximation the two channels were associated with the same decay rates, for times much shorter than the thermalization time. For high temperature reservoirs, when the decay rate for transition up channel was temporarily negative, it means that the channel is operating in reverse direction, i.e., due to the reservoir memory, the information that went from the system into the reservoir feeds back into the system. A particularly interesting behavior occurs in the super Ohmic resonant case at zero temperature. In this case, indeed, our results show that the thermalization process takes place via the reversed transition up channel.

We also examined the heating function for short and long time scales. At short times the non-Markovian dynamics of the heating function may be characterized by oscillations indicating that the system gives back to the reservoir some of the energy it had obtained previously. In the long time limit the thermalization times strongly depend, as expected, on the reservoir type and on the resonance factor r. The off resonant reservoirs heat up the systems considerably slower than the resonant reservoirs. We observed a clear connection between the heating function dynamics and the reservoir spectral density. For all types of reservoir spectra, the

low frequency part of the spectrum induces oscillations, while the high frequency part is responsible for the Markovian monotonic heating.

The results obtained in this thesis pave the way to the study of the possible influence of the reservoir spectrum on the occurrence of Zeno or anti-Zeno effect. The Zeno effect is the inhibition of the decay of an unstable/open quantum system due to a series of measurements aimed at checking whether the system is still in its initial state or not [28]. The quantum Zeno effect predicts that, under certain conditions, the more frequently the measurements are performed, the slower is the system decay. In theory, by performing continuous measurements, one would be able to stop the decay completely. In some cases, however, measurements give rise to an anti-Zeno effect, i.e., the acceleration of the system decay. The borderline between the occurrence of the Zeno or anti-Zeno effect is characterized by the spectrum of the environment through decay coefficient $\Delta(t)$. A comparative study of the Zeno-anti-Zeno crossover is thus a natural follow-up of this thesis.

Bibliography

[1] Quantum Approach to Informatics, S. Stenholm, K.-A. Suominen, (Wiley, New Jersey, 2005)

[2] Preferred sets of states, predictability, classicality, and environment-induced decoherence, W. H. Zurek, in Physical Origins of Time Asymmetry (Cambridge University Press, Cambridge, 1994)

[3] W. H. Zurek, Rev. Mod. Phys. **75**, 715 (2003), C. Monroe *et al.* Phys. Rev. Lett. **77**, 4281 (1996), S. Haroche, J.-M. Raimond, Physics Today **49**, 51 (1996)

[4] E. Schrödinger, Naturwissenschaften **23**, 807, 823, 844 (1935), English translation by J. D. Trimmer, Proceedings of the American Philosophical Society **124**, 323 (1980)

[5] The Theory of Open Quantum Systems, H-P. Breuer, F. Petruccione, (Oxford University Press, Oxford, 2002)

[6] J. R. Anglin, W. H. Zurek, Phys. Rev. D **53**, 7327 (1996)

[7] W. H. Zurek, Rev. Mod. Phys. **75**, 715 (2003)

[8] I. Joichi, Sh. Matsumoto, M. Yoshimura, Phys. Rev. A **57**, 798 (1998)

[9] P. Hänggi, P. Talkner, M. Borkovec, Rev. Mod. Phys. **62**, 251 (1990)

[10] D. Leibfried, R. Blatt, C. Monroe, D. Wineland, Rev. Mod. Phys. **75**, 281 (2003)

[11] F. Intravaia, S. Maniscalco, A. Messina, Eur. Phys. J. B **32**, 97 (2003)

[12] Quantum Optics, M. O. Scully, M. S. Zubairy, (Cambridge University Press, Cambridge, 1997)

[13] J. Piilo, S. Maniscalco, Phys. Rev. A **74**, 032303 (2006)

[14] Solid State Physics, N. Ashcroft, D. Mermin, (Saunders College Publishing, Philadelphia, 1976)

[15] A. O. Caldeira, A. J. Leggett, Phys. A **121**, 587 (1983)

[16] B. L. Hu, J. P. Paz, Y. Zhang, Phys. Rev. D **45**, 2843 (1992)

[17] J. B. Paz, W. H. Zurek, in Coherent Matter Waves, Proceedings of the 72nd Les Houches Summer School (Springer-Verlag, Berlin, 1999)

[18] Quantum Noise, C. W. Gardiner, (Springer-Verlag, Berlin, 1991)

[19] F. Intravaia, S. Maniscalco, A. Messina, Phys. Rev. A **67**, 042108 (2003)

[20] Quantum dissipative systems (2nd edition), U. Weiss, (World scientific publishing, Singapore, 1999)

[21] J. J. Hope, G. M. Moy, M. J. Collett, C. M. Savage, Phys. Rev. A **61**, 023603 (2000)

[22] T. Quang, M. Woldeyohannes, S. John, G. S. Agarwal, Phys. Rev- Lett. **79**, 5238 (1997)

[23] O. Astafiev, Yu. A. Pashkin, Y. Nakamura, T. Yamamoto, J. S. Tsai, Phys. Rev. Lett. **96**, 137001 (2006)

[24] Photonic crystals: molding the flow of light, J. D. Joannopoulos, R. D. Meade, J. N. Winn, (Princeton University Press, Princeton, 1995)

[25] P. M. V. B. Barone, A. O. Caldeira, Phys. Rev. A **43**, 57 (1991)

[26] A. Shnirman, Y. Makhlin, G. Schön, Phys. Scr. **T102**, 147 (2002)

[27] J. Piilo, S. Maniscalco, K. Härkönen, K.-A. Suominen, Phys. Rev. Lett. **100**, 180402 (2008)

[28] S. Maniscalco, J. Piilo, K.-A. Suominen, Phys. Rev. Lett. **97**, 130402 (2006)

[29] S. Maniscalco, J. Piilo, F. Intravaia, F. Petruccione, A. Messina, Phys. Rev. A 70, 032113 (2004)